IN SITU ^{13}C NMR MONITORING OF THE DEHYDRATION OF 2-PROPANOL OVER H-ZSM-5

by

David Rees Morgan

Thesis submitted to the Faculty of the
Virginia Polytechnic Institute and State University
in partial fulfillment of the requirements for the degree of

MASTER OF SCIENCE

in

Chemistry

APPROVED:

H. C. Dorn, Chairman

H. M. Bell

M. E. Davis

February, 1989

Blacksburg, Virginia

In Situ ^{13}C NMR Monitoring of the dehydration of 2-Propanol over H-ZSM-5

by

David R. Morgan

Committee Chairman: Harry C. Dorn
Chemistry

(ABSTRACT)

The first in situ ^{13}C NMR monitoring of zeolite catalyzed reaction is described. The dehydration of 2-propanol over H-ZSM-5 was observed using solution type techniques. Although this produces broad lines, several mechanistic details were elucidated. This study indicates that: 1) the dehydration does not proceed through a cyclopropyl carbenium ion intermediate, 2) propene oligomerizes on the catalyst and reaches a steady state concentration before propene is desorbed, and 3) the 2-propanol flowing over the catalyst does not react with the oligomerized propene.

Acknowledgements

I would like to thank my research director, Dr. Harry Dorn, for his patience, support and guidance. A also want to thank Dr. Mark Davis who provided the catalyst, some background references, and who answered my many questions about H-ZSM-5. I appreciate the help of Mr. who taught me how to use the NMR and helped me with any experimental problems. Finally, I would like to thank my fellow graduate students who assisted me somewhere along the way and kindly answered my thousands of questions.

Table of Contents

List of Figures

List of Figures (cont.)

List of Figures (cont.)

List of Tables

Introduction

Zeolites and their role as catalysts have been widely studied by numerous analytical techniques. Many of the early studies utilized adsorption-desorption and various thermal techniques to determine their acid-base properties. Gas chromatography has been used to look at product distributions under various operating conditions. While these studies have produced much practical information, they do not explicitly reveal the reaction mechanism. The best one could do is to deduce a mechanism that is consistent with the data. Gradually, techniques that reveal what is actually going on inside the catalyst, such as FTIR and photoacoustic spectroscopy have been successfully employed. While these techniques have added enormously to our understanding of catalysts they are still limited by overlapping peaks and they do not provide information about the existence of carbocations. The next logical step in the understanding of the catalysts was the application of NMR. With NMR one may monitor the nuclei of the catalyst or of the reacting species. NMR also may provide dynamic information as well as chemical information of the analyte. A real boon to the study of catalysts has been the development of cross-polarization and magic-angle spinning techniques. These techniques improve the sensitivity and the line widths. Most of the CP-MAS studies were essentially batch processes where an analyte was adsorbed and then analyzed. This suffers from the drawback that reactions often occur before the catalyst can be analyzed, and often only a low concentration of reactant molecules may be introduced into the system.

In the present studies, we felt improvements were possible if the sample could be monitored continuously in a flowing stream, rather than in a batch process. In situ NMR monitoring has the following advantages: 1) The flowing system is a better approximation to a "working" catalyst, 2) the catalyst can reach a steady-state condition, 3) at a steady-state condition sampling times can be increased to enhance signal to noise, and 4) the products can be continuously monitored.(*1*)

This thesis describes the first use of in situ NMR, by solution type techniques, in the monitoring of a zeolite catalyst. Specifically we will examine the dehydration of 2-propanol on the industrially important catalyst, H-ZSM-5. The first chapter is devoted to the background and theory of H-ZSM-5 and flow and solid-state NMR. Chapter 2 describes the instrumentation and the experimental procedure. Chapter 3 covers the results and discussion section and the conclusion summarizes the results and contains suggestions for future studies.

CHAPTER 1

History and Theory

Introduction to Zeolites

Zeolites are crystalline aluminosilicates that contain water and exchangeable metal cations, usually alkali or alkali-earths within their framework. Zeolites were discovered in 1756 by A. F. Cronstedt, who coined the term zeolite because they boil and swell when heated. (From the Greek zein = to boil and lithos = stone). There are over 30 naturally occurring zeolites and the number of synthetic zeolites is over 100 and still increasing.(*2*)

Zeolites may be describe by the empirical formula:

$$M_{2/n}O \cdot Al_2O_3 \cdot x\ SiO_2 \cdot y\ H_2O$$

where $x \geq 2$ because two alumina tetrahedra may not be adjacent to one another. An alternative and perhaps better description of a zeolite can be given by the structural formula for the unit cell:(*3*)

$$M_{z/n}[(AlO_2)_z\ (SiO_2)_y] \cdot w\ H_2O$$

where n = cation valence, w = number of water molecules and (x + y) = the total number of tetrahedra in the unit cell. Many of the special properties of zeolites can be understood by examining the structure. The structural framework consists of SiO_4 and AlO_4 tetrahedra that share oxygen atoms. This produces a system of interconnecting channels within the zeolite. Residing in these channels are the adsorbed water and the cations which are required to make the zeolite electrically neutral. Many zeolites are used as dehydrating agents because

they can lose this water reversibly. They may also be used as cation exchangers because the cations are loosely held and may be exchanged by other cations. These channels have such a high surface area that when a zeolite is dehydrated, over 90 % of the total surface area may be internal. Zeolites are also referred to as molecular sieves because small molecules can be separated by size and shape by the rigid porous network.(*4*)

While the previously mentioned uses of zeolites have some commercial value, their use a as catalysts far surpasses any other use. Most of the zeolite catalysts used today are synthetic because they must often have a high purity and clearly defined structure to be effective. A discussion of the synthetic zeolites and, in particular, H-ZSM-5 follows.

H-ZSM-5 (Background and Structure)

The first synthetic zeolite, Linde type A, was developed at Union Carbide in 1949.(*4*) This led to a boom in the synthesis of zeolites with the patent for ZSM-5 being granted in 1972.(*5*) The letters ZSM represent Zeolite Socony Mobil. This catalyst has generated much interest because only certain molecules may fit into its porous network. As with zeolites in general, an understanding of the framework is critical in understanding how it functions as a catalyst.

The framework consists of SiO_4 and AlO_4 tetrahedra joined together in five member rings called pentasil units. The pentasil units are joined to form chains or columns. (Figure 1.1) The resulting columns can be joined to each other several ways. When the pentasil layers are related by an inversion symmetry operation, the framework is that of ZSM-5.(*6*) (Figure 1.2) The framework has two different types of channels penetrating the structure. (Figure 1.3) One of the channels is straight with elliptical openings of 0.51 x 0.58 nm and the other has nearly circular openings of 0.54-0.56 nm and is in a zig-zag or sinusoidal form. The intersection of these channels creates a cavity approximately 0.8 nm in diameter.(*7*) It is in the cavities where much of the catalytic chemistry occurs.

ZSM-5 is not one zeolite but actually a family of zeolites that meet the following criteria:

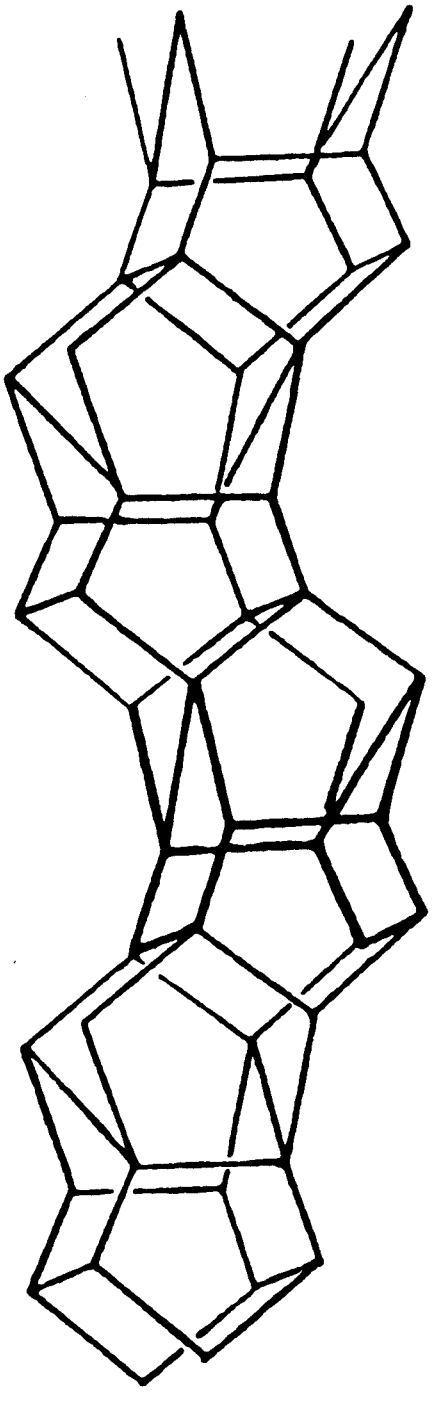

Figure 1.1 Column of pentasil units which is a building block of ZSM-5 structure.

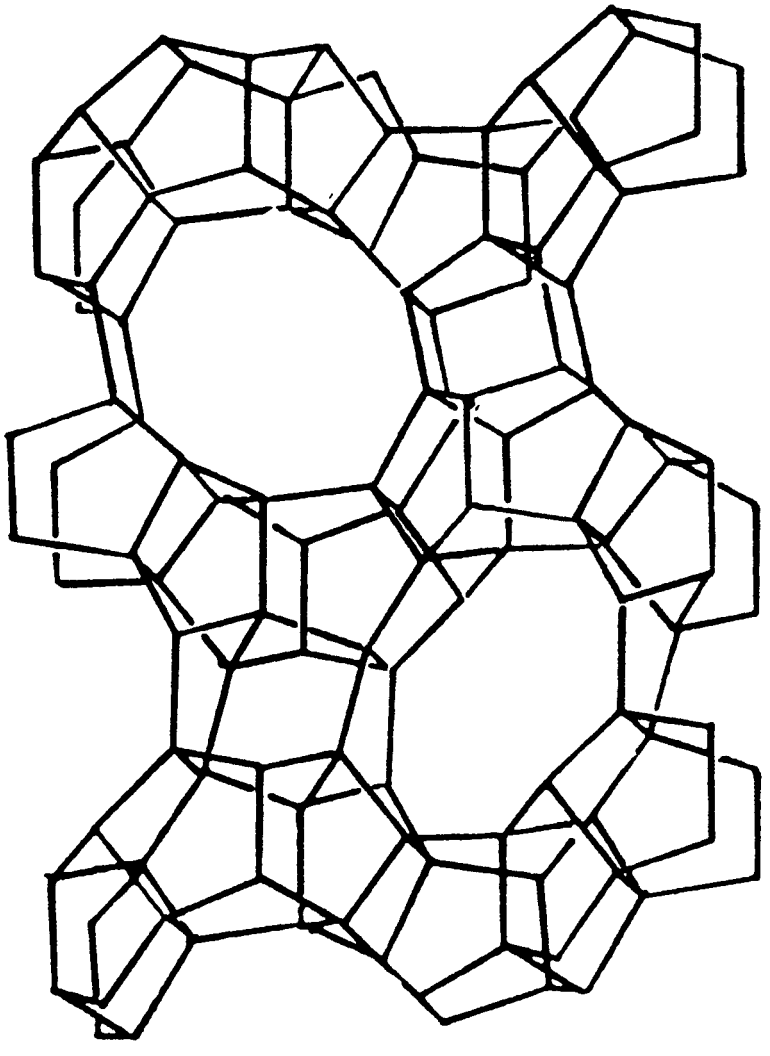

Figure 1.2 Crystal lattice of ZSM-5.

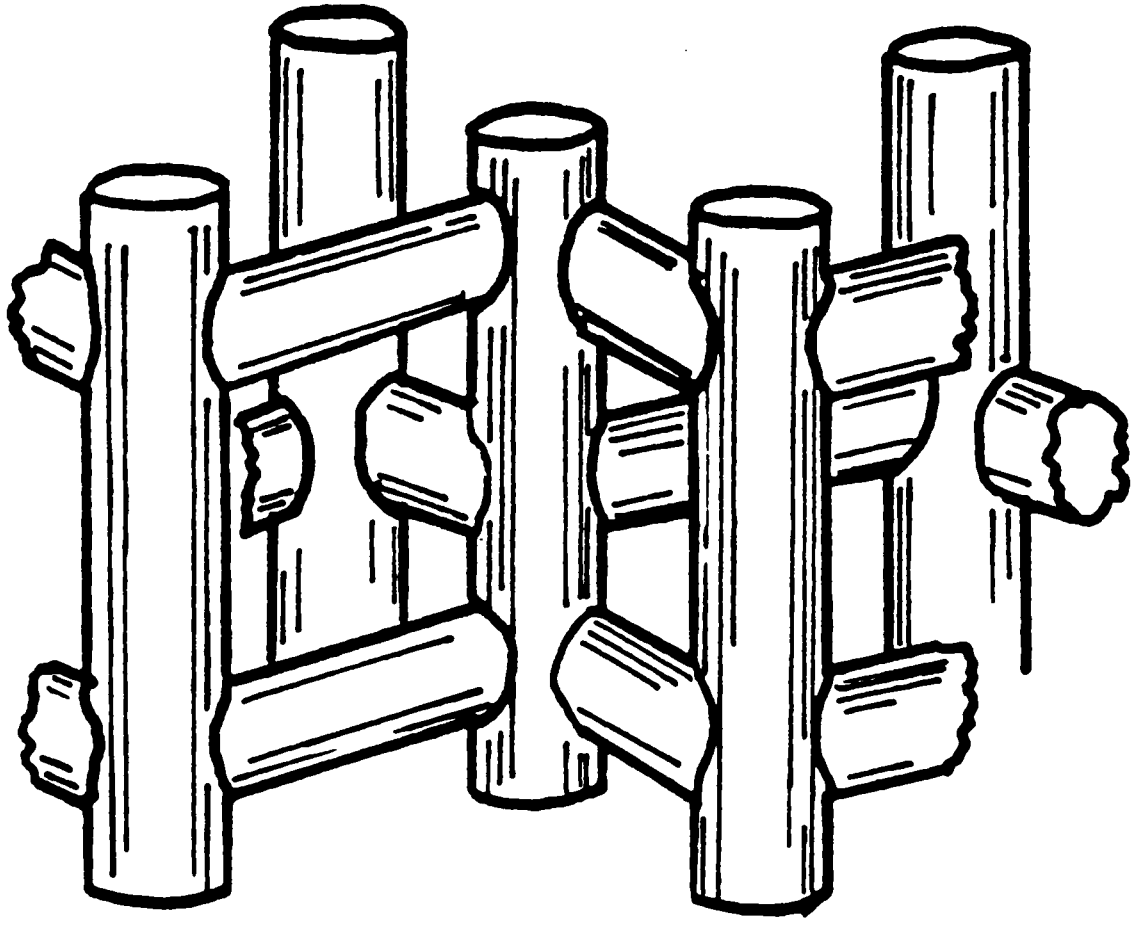

Figure 1.3 Channel structure of ZSM-5.

1) they have a particular x-ray diffraction pattern, 2) they have a silica to alumina ratio of greater than 12 and 3) they have a constraint index between 1 and 12 (a typical value is 8.3). The constraint index shows the relative cracking rate of two hydrocarbons and is defined as:(*7*)

$$\text{constraint index} = \frac{\log(\text{fraction of hexane remaining})}{\log(\text{fraction of 3-methyl pentane remaining})}$$

More recently, two other methods have been developed to clearly identify ZSM-5. One method compares the IR absorbance at 550 cm^{-1} to the band at 460 cm^{-1}. If the ratio is greater than 0.8, the zeolite is considered pure.(*8*) The other technique is to use ^{29}Si MAS-NMR because the ZSM-5 has a distinctive spectrum for both the monoclinic and orthorhombic forms.(*9*)

The synthesis of ZSM-5 has been thoroughly investigated and there are many procedures in the literature.(*6*) Although the particular details vary, the general recipe for the synthesis of ZSM-5 includes: sodium oxide, alumina, silica, water and a tetrapropylammonium compound, (TPA). The TPA is very important because it acts as a template for the creation of the intersecting channels. Once the zeolite is formed, it contains exchangeable sodium ions. The acid form of ZSM-5 can be made by exchanging the sodium ion with a proton from an acid solution. An alternative approach is exchanging the sodium for an ammonium ion and heating to liberate ammonia and leaving a proton behind in the lattice. The acid form, designated H-ZSM-5, is a strong acid catalyst that has been used for a wide variety of processes including alkylation of aromatics, isomerizations, and the conversion of methanol to gasoline. Since H-ZSM-5 is widely used in the petroleum industry there has been significant financial impetus to understand the chemistry of this catalytic system. The next section will review some of the literature concerning the nature of the acidity and the mechanism of catalysis.

Catalytic Studies Utilizing H-ZSM-5

H-ZSM-5 has strong acidic properties and is capable of catalyzing reactions requiring strong acids such as Friedel-Crafts alkylations and the dehydration of alcohols. Many of the early studies involved describing the nature of the acidic sites. The density and the nature of the acidic sites were determined by thermogravimetric analysis, TGA, and the adsorption-desorption of basic molecules. The main source of acidity is the OH group which acts as a Bronsted acid rather than the Al site acting as a Lewis acid. Even though the catalyst may be described as a Bronsted acid, this is not a complete description because the zeolite structure plays a significant role in acidity.(*10*) One approach to understanding the nature of the acidity is to monitor model reactions, such as the dehydration of an alcohol. Grady and Gorte(*11*) used temperature programmed desorption, (TPD), TGA, and transmission infrared spectroscopy to study the adsorption of 2-propanol and propene on H-ZSM-5. They found that above 360 K one 2-propanol molecule remains on the catalyst for each hydrogen cation. This adsorbed species reacts with gas phase propene to form hexenes and nonenes. They also found that deuterium was incorporated into the molecule when propene was adsorbed on D-ZSM-5. These results led them to conclude that the dehydration of 2-propanol proceeds via a carbenium ion intermediate. Ghosh and Kidd(*12*) used FTIR to study the formation of coke on acidic zeolites. This work showed that the Bronsted sites are important for coke formation, but H-ZSM-5 resists coke formation even though it is strongly acidic. Anderson, Mole, and Christov(*13*) used GC-MS and deuterium labelling in the study of the alkylation of benzene over H-ZSM-5 and concluded that the alkylations were Bronsted acid catalyzed electrophilic substitutions.

While these experiments showed indirect evidence of carbenium ion formation, a carbenium ion had not been spectroscopically observed. One method that has the potential to prove the existence of a cation is NMR. NMR also has the advantages of giving structural and dynamic information about the carbenium ion and its interactions with the lattice. Zardkoohi, Haw and Lunsford(*14*) examined the adsorption of propene on an HY catalyst

using ^{13}C CP-MAS NMR and found a peak at 250 ppm which they attributed to an isopropyl cation. One disadvantage of this system is that it is not an in situ technique, and much care must be taken in preparing the sample.

Very recently, both Gore et al(*15*) and Haw et al(*16*) revised their carbenium ion hypotheses. Gore et al used ^{13}C MAS NMR to study the dehydration of 2-methyl-2-propanol, (^{13}C at the 2 position). No carbenium ion was observed, and they proposed that the active intermediate was an alkoxide which exhibited a resonance at 77 ppm. Using ^{13}C CP-MAS, Haw et al concluded that the active intermediate produced from the adsorption of propene of HY was also an alkoxide. Their hypothesis suggests that the peak observed at approximately 250 ppm was due to a substituted cyclopentenyl cation which could be formed from the reaction of two or three propene molecules. They reasoned that the cation would have an appreciable lifetime because of steric and electronic features.

There are two approaches to the NMR study of zeolites. One method is to monitor the reacting molecule and the other is to monitor a species that does not participate in the reaction but is sensitive to structural and electronic effects of the catalyst. The second method, using ^{129}Xe, was pioneered by Fraissard and coworkers.(*17,18,19*) When monitoring a reactant molecule of limited mobility, as in our studies, solid-like interactions should be considered and these are explained in the next section.

Theory of Solid State NMR

Since solution type techniques will be used with a primarily solid sample a complete understanding of the interactions of a nucleus in the solid state is necessary to make appropriate choices for the spectral parameters.

The interactions of a nucleus with a magnetic moment are much more complex in the solid state than in solution NMR. The possible interactions in the solid state are:(*20*)

1) The Zeeman interaction with the magnetic field.

2) Direct dipole-dipole interactions with other nuclei.

3) Magnetic shielding by the surrounding electrons giving chemical shifts.

4) Spin-spin couplings to other nuclei.

5) Quadrupolar interactions which will be present for nuclei with spin > 1/2.

These interactions may be expressed in the general form of the spin Hamiltonian as:

$$H = H_z + H_d + H_{cs} + H_{ss} + H_q$$

The approximate ranges of the different spin interactions are given in Table 1.1. Each interaction and how it relates to our study of H-ZSM-5 will now be considered in detail.

Zeeman interaction, (H_z), occurs for all nuclei with a magnetic moment. The interaction of the magnetic field, H_o, with the magnetic moment produces (2I + 1) energy levels, with the separation between energy levels

$$E = \hbar w_o = \gamma \hbar H_o$$

The Hamiltonian may be written as:

$$H_z = -\gamma \hbar H_o I_z = -g_n \beta_n H_o I_z$$

where I = nuclear spin quantum number, γ is the magnetogyric ratio, w_o is the corresponding Larmor frequency, g_n is the nuclear g factor and β_n is the Bohr magneton for the particular nucleus. This interaction is linear with the applied magnetic field so a larger field produces a larger energy difference between energy levels which in turn creates a larger population difference and ultimately improves the S/N. This interaction is present in both the solution and solid state spectra. The Zeeman interaction is also proportional to the magnetogyric ratio, γ. If this was the only interaction in our system, the monitoring of ^1H, with its larger magnetogyric ratio would be preferred over ^{13}C, but as will be seen shortly, there are resolution problems with monitoring ^1H.

Table 1.1

Approximate ranges of the different spin interactions (in Hz)

Zeeman	10^6-10^9
Dipolar	0 -10^5
Chemical Shift	0 -10^5
Scalar Coupling	0 -10^4
Quadrupolar	0 -10^9

Dipolar interactions, (H_d), arise from the direct dipole-dipole interactions between nuclei. The Hamiltonian for the dipolar interaction between an isolated pair of spins I and S may be expressed:

$$H_D = H_{IS} = \frac{\gamma_I \gamma_S \hbar^2}{r_{IS}^3} \vec{I} \cdot \hat{D} \cdot \vec{S}$$

where r_{IS} is the internuclear distance and D is the dipolar coupling tensor. The total interaction will be the summation of all possible pairwise interactions. It should be noted that the interaction depends on γ so this interaction will be particularly important for spin 1/2 nuclei with large magnetic moments, (^1H, ^{19}F, ^{31}P). This interaction is independent of the applied field, H_0, and it falls off rapidly with internuclear distance. For typical homonuclear ^1H systems the dipolar interactions range up to 40 kHz, where as ^1H-^{13}C interactions are usually half that value and ^{13}C-^{13}C dipolar are roughly ten times smaller. The dipolar coupling tensor, D, can be expressed as a 3x3 matrix. When this matrix is diagonalized by changing coordinate systems, it can be shown that the dipolar interaction has a dependence of $(1 - 3\cos^2\theta)$, where θ is the angle between the magnetic field and the internuclear vector r_{ij}. If the sample is tilted 54.7° with respect to the magnetic field the term $(1 - 3\cos^2\theta)$ goes to zero and the dipolar interaction diminishes. In a liquid with isotropic tumbling, the dipolar interaction is zero. In a solid sample with adsorbed species the adsorbed species have limited motion so the dipolar interactions will not be eliminated. Since our in situ experiment cannot be spun at the magic angle, we have to monitor a nucleus other than ^1H because the proton dipolar couplings would dominate the spectra. The dipolar interaction will also be reduced at higher temperatures because of increased motion of the adsorbed species.

Chemical shift interaction, (H_σ), is due to the shielding effect on the nucleus by the fields produced by the surrounding electrons and is described:

$$H_\sigma = \gamma_I \hbar \vec{I} \cdot \hat{\sigma} \cdot \vec{H}$$

This is also proportional to the applied field. The interaction is very sensitive to the geometry and identity of other atoms surrounding the nucleus. In solution NMR, where there is rapid isotropic motion, the chemical shift is averaged and produces a one line spectrum. In the solid-state there is a geometric dependence and each orientation can give rise to a different chemical shift. The chemical shift tensor, like D, also has an angular dependence and at the magic angle of $\theta = 54.7°$ it can be shown that the chemical shift produces an average value just as a solution would. Since the adsorbed species will have some motion, but not isotropic motion, the chemical shift should be partially averaged creating broad lines.

Spin-spin coupling, (H_{ss}). The interaction between a pair of spins, I and J is expressed:

$$H_{ss} = \vec{I} \cdot \hat{J} \cdot \vec{S}$$

This interaction, which is field independent, occurs in both liquid and solid state, and the interaction may be eliminated by heteronuclear decoupling.

Quadrupolar interaction, (H_q), is only for nuclei with $I > 1/2$. The Hamiltonian is:

$$H_q = \vec{I} \cdot \hat{Q} \cdot \vec{I}$$

This effect arises from the interaction of the nuclear electric quadrupole moment, eQ, with the non-spherically symmetric field gradient around the nucleus. The broadening can be reduced by MAS but since our system cannot be spun, the spectra would be completely dominated by quadrupolar broadening. Quadrupolar broadening prevented us from studying nuclei such as ^2H.

Summarizing the effects one should see from a static solid with adsorbed species of limited motion: If ^{13}C is monitored with ^1H decoupling there will be broadening of the lines from ^{13}C-^1H dipolar interactions and chemical shift anisotropy that is not completely averaged.

FLOW NMR-APPLICATIONS AND THEORY

In addition to the adsorbed species on the catalyst there should be species that have high mobility that are flowing through the catalyst. To understand the detection problems with these species requires some background on flow NMR, which this section describes.

Flow NMR is analogous to solution NMR except the analyte flows through the observation region. The early applications of flow NMR involved measuring flow rates and studying the dynamics of flow. In 1951, Suryan(*21*) performed the first flow NMR experiment when he monitored a flowing aqueous solution of $FeCl_3$ and showed that the signal intensity was proportional to the flow rate. The increased intensity was explained by the influx of new polarized nuclei into the detector. In 1959, Singer used NMR to measure the blood flow in mice(*22*) and later applied the technique to human blood flow.(*23*) A spin-echo technique was used to study the velocity distribution pattern in liquids,(*24*) and for the measurement of diffusion in liquids.(*25,26*) In the 1970's Fyfe describe a flow system(*27*) and its application in the study of transient organic intermediates and chemical kinetics.(*28,29*) With the advent of FTNMR, higher magnetic fields, and the resulting increases in sensitivity, flow NMR was applied as an on-line detector for HPLC(*30,31,32*) and GC.(*33*) In the early 1980's, Dorn et al developed toroid shaped cells for signal enhancement(*34,35*) and they discussed conditions for quantitative flow FT-^{1}HNMR under repetitive pulse conditions.(*36*)

To optimize the conditions of flow NMR one must understand how a flowing stream and a non-spinning cell affect resolution and the signal to noise ratio, S/N. In flow studies the sample tube does not spin which reduces the magnetic field homogeneity and leads to a reduction in resolution and S/N. The loss in resolution is, however, relatively small for modern spectrometers. The major loss in resolution is usually due to flow.(*20*) The line width at half-height can be expressed:

$$\Delta\nu_{1/2} = \frac{1}{\pi T_2(\text{obs})}$$

and the broadening due to flow can be written:

$$\frac{1}{T_2(obs)} = \frac{1}{T_2(stat)} + \frac{1}{\tau}$$

where $T_2(obs)$ is the actual T_2,the spin-spin relaxation time, which determines the linewidth, and τ is the residence time of the sample in the measuring coil. As the flow is increased, $1/\tau$ makes a larger contribution to the linewidth. A plot of the linewidth versus the flow rate should produce a straight line with the intercept equal to $1/T_2(stat)$.(*27*) In a manner similar to T_2, the spin-lattice relaxation time, T_1 also changes in a flowing system. The expression for T_1 is:(*37*)

$$\frac{1}{T_1(obs)} = \frac{1}{T_1(stat)} + \frac{1}{\tau}$$

At high flow rates, $1/\tau$ dominates and $1/T_1(obs)$ becomes larger. As $T_1(obs)$ decreases, the pulse repetition rate can be increased to improve S/N. As illustrated by the equations for T_1 and T_2, flow NMR presents a tradeoff of resolution for S/N, however, this is often useful for a nucleus with a wide shift range such as ^{13}C, ^{19}F, ^{31}P.

There are several practical experimental aspects that must be considered before initiating a flow NMR experiment. If the concentration of the nucleus of interest is very low, as in the case of natural abundance ^{13}C, the molecule may need to be labelled or the system may need to flow through the detector for a long time. For non-reacting systems this is not a problem because the flow can be recycled, but for reacting species this may require a lot of starting material. Inclusion of a deuterium containing compound may be expensive in a flow system, therefore, an external lock standard may sometimes be employed. For shorter experiments, no lock at all may be necessary for high resolution superconducting solenoids. A third and very important consideration is premagnetization of the sample. To maximize a signal, the nuclei should reside in the field at least 5 T_1's. At low flow rates, no modification may be

necessary because most magnets have a large magnetic field for several centimeters outside the observation region. However, fast flow rates may require extra volume, (e.g. extra coiled tubing), before the observation region to provide sufficient time for premagnetization.

CHAPTER 2

Experimental

Experimental apparatus

A schematic diagram of the apparatus is presented in figure 2.1. Nitrogen gas at 2.5 psi flowed through a Matheson flow controller set to operate at 10 ml/min. The nitrogen went through a splitter so that the flow could go directly to the catalyst or it could be diverted to flow through a glass bubbler that contained the 2-propanol. The bubbler was connected to the apparatus with Teflon® tubing. The reaction cell containing the catalyst was a glass tube 160 mm long and 12 mm in diameter with a glass frit in the bottom to allow the passage of gases. The reaction cell was attached to the Teflon® tubing with a Teflon® screw cap and a rubber o-ring to provide a good seal. The gases would flow out the bottom of the reaction vessel and through more Teflon® tubing which led to either a CCl_4/Br_2 trap or to a gas chromatograph and then to the CCl_4/Br_2 trap. The flow and most of the static NMR spectra were run on a JEOL FX-200 using quadrature detection. The probe was tuned to 50.10 MHz. The gas chromatograph was a Varian 90-P operated isothermally, with Helium carrier gas, and thermal conductivity detection. The 1/8" i.d. x 4.5 ft. column was packed with 80-100 mesh Poropak T. The effluent sampling was done with a Valco liquid chromatography sampling valve with a 2 ml sample loop. The chromatograms were recorded with a linear instruments integrating chart recorder.

The accuracy and lag time of the variable temperature system were tested by placing a copper-constantan thermocouple in the zeolite bed and placing it in the probe. The temperature reading of the instrument was accurate and the zeolite would reach the temperature in less than 1/2 hour.

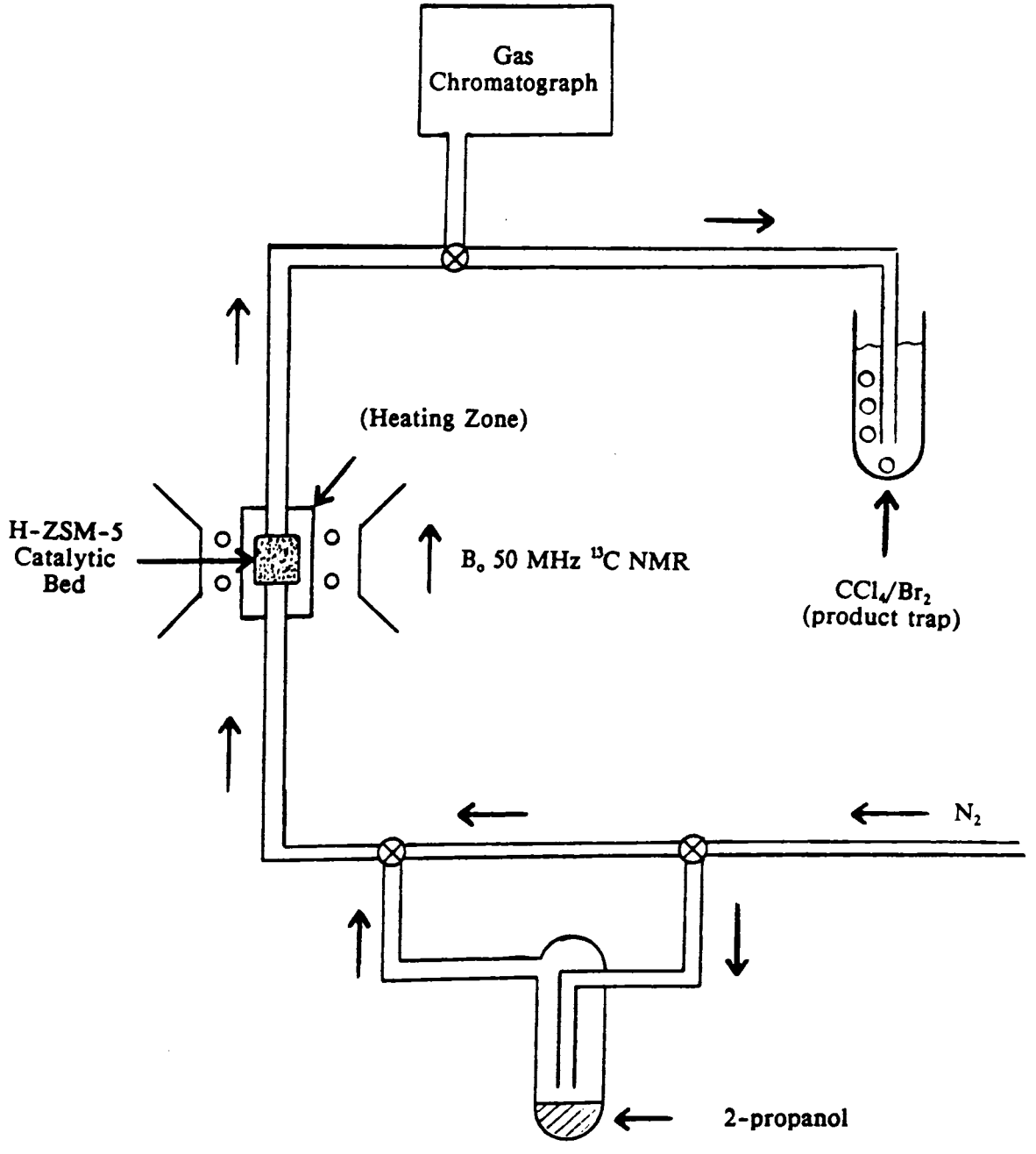

Figure 2.1 **Schematic of flow NMR apparatus.**

Synthesis of ^{13}C labelled 2-propanol

Since our flow system did not have high sensitivity, labelled 2-propanol was necessary to achieve an adequate signal. The preparation of the labelled 2-propanol followed the reaction scheme below:

$$Ba^{13}CO_3 + H_2SO_4 \longrightarrow BaSO_4 + {}^{13}CO_2 + H_2O$$

$$^{13}CO_2 + CH_3MgBr \xrightarrow{H+} CH_3{}^{*}COOH$$

$$CH_3{}^{*}COOH + LiOH \longrightarrow CH_3{}^{*}COOLi$$

$$2\ CH_3{}^{*}COOLi \xrightarrow{500^\circ} CH_3{}^{*}COCH_3 + LiCO_3$$

$$CH_3{}^{*}COCH_3 + NaBH_4 \longrightarrow CH_3{}^{*}C(OH)HCH_3$$

30 g of $Ba^{13}CO_3$ was placed in a round bottom flask fitted with a dropping funnel containing 250 ml of concentrated H_2SO_4. Tygon tubing connected the top of the dropping funnel to another round bottom flask fitted with a stopcock and containing, 85 ml of 3.2 M CH_3MgBr and 200 ml of anhydrous ethyl ether. The whole system was attached to a vacuum system with a manometer. The Grignard solution was frozen in liquid nitrogen and the system was evacuated to approximately 1 mm. The system was shut off from vacuum and the Grignard was warmed until the solid was broken up and could be stirred. While keeping the Grignard solution between -30 and -40° C the H_2SO_4 was added dropwise to the $Ba^{13}CO_3$ over a period of 2 hours. The Grignard solution was stirred for one more hour then slowly acidified with 6N HCl until pH 1. The ether was distilled, and the water layer was then distilled and the acid combined with the ether. The ether/water/acetic acid solution was neutralized with LiOH to the phenolphthalein endpoint with the ether and most of the water removed by distillation and the lithium acetate was thoroughly dried in an evaporating dish. The resulting pink solid, (9 g), was crushed into a fine powder and evenly distributed in a pyrolysis tube. The pyrolysis tube was connected to a gentle stream of nitrogen and the lithium acetate was heated to 500° C over the course of 90 minutes. The liberated acetone was collected in two dry ice-acetone traps. The contents of the first trap was added dropwise

to a solution of 0.95g of $NaBH_4$ in 20 ml of freshly distilled diglyme and stirred overnight. The solution was cooled with ice and acidified with 2 ml of water. The product mixture was then distilled using a short path apparatus producing approximately 2.5 ml of 2-propanol. The only contaminant in the final product was water which was adsorbed using 3 Å molecular sieves.

Monitoring of H-ZSM-5

One gram of white H-ZSM-5 (Si/Al = 60) was placed in the flow cell with a small plug of glass wool on top of the catalyst. The catalyst completely filled the detector region in the NMR. The flow cell was placed in the magnet, the flow on N_2 started and ^{13}C spectra were taken at room temperature and 180° C. No peaks were visible in the observed range of -30 to 370 ppm. In all subsequent experiments, the catalyst was pretreated by heating it above 100° C under flowing dry nitrogen in the NMR cell for over one hour. A drop of 2-propanol was placed on the catalyst at room temperature and the flow of N_2 continued to distribute the alcohol. The high concentration of alcohol was used to find the spectral parameters. A 90° pulse was found by varying the pulse duration between 10 and 85 microseconds with the optimum being 27.5 microseconds. The longitudinal relaxation time, T_1, was measured using 180 - τ - 90 pulse sequence with τ being varied between 1 and 14 milliseconds with τ_{null} = 8 milliseconds which corresponds to a T_1 of (8 milliseconds/ln 2) = 11.5 milliseconds. Since real time monitoring was important the spectra had to be maximized over a period of time. To accomplish this a variety of relaxation delays and number of scans were tried to maximize the signal in a 10 minute period. The conditions that were employed for most of the spectra are given in table 2.1. Since we were interested in sensitivity rather than resolution we used zero-filling and a large value for the line-broadening.

After the spectral parameters were determined the catalyst was heated slowly from room temp to 180° C over the course of 11 hours. Spectra were collected every 10 minutes. During the experiment, one spectrum with a pulse delay of .25 seconds was run, but this showed little improvement over the other spectra. At the end of the run the nitrogen gas was turned on

Table 2.1

Flow NMR Spectral Parameters

Observation frequency	50.10 MHz
Pulse width	20 μsec
Spectral width	20,000 Hz
Number of points	4096
Number of sample points	1920
Obset	87.00 KHz
Acquisition time	48 ms
Pulse delay	12 ms
Number of scans	10,000
Noise decoupling	199.50 MHz

to see if the products would desorb.

The second set of experiments was similar except that the 2-propanol flowed through the apparatus in the nitrogen stream. The temperature range was confined to 100 - 130° C and the effluent was bubbled into NMR tubes containing CCl_4/Br_2 solution. These traps were changed every half hour. Toward the end of the experiment the nitrogen gas bypassed the 2-propanol bubbler and flowed directly to the catalyst. The collected products were analyzed using high resolution ^{13}C NMR. The third set of experiments was an isothermal run at 180° C. The alcohol in nitrogen was flowed over the catalyst at about 19 ml/min. The product traps were changed at various times and after the catalyst appeared to reach a steady-state the flow to the alcohol was switched on and off several times and the resulting spectra monitored. Also, one spectrum with a 1 second pulse delay was run to check for slowly relaxing species. The used catalyst was examined by solid-state ^{13}C NMR both with and without cross polarization.

The fourth set of experiments included several improvements: inclusion of an internal reference, analysis of products by gas chromatography and a dual bubbler was used so that both labelled and non-labelled 2-propanol could be used in the same experiment. The internal standard was formamide because it has a high boiling point, it has only one carbon with a short T_1, and its chemical shift 165.5 (*38*) does not overlap with any expected resonances. The formamide was placed in a sealed capillary and the capillary was attached to the catalyst cell with teflon tape. The effluent passed through a 2 ml gas sampling loop and then into the CCl_4/Br_2 trap. Chromatograms were taken approximately every eight minutes and the collected products were analyzed by both ^1H and ^{13}C solution NMR on a Bruker 270 MHz spectrometer. This experiment was isothermal at 130° C and several trial runs with non-labelled 2-propanol were done to test the chromatography and to see if any signal could be seen from the non-labelled 2-propanol. Since the non-labelled alcohol produced very weak signals, ^{13}C labelled 2-propanol was flowed over the catalyst until it appeared to reach steady state then the bubbler was switched to non-labelled 2-propanol.

CHAPTER 3

Results and Discussion

To adequately describe and interpret our results, it is necessary to have an understanding of the probable reactions of 2-propanol on a strong acid catalyst. From previous studies (*11,12,15,39,40*) and analogies to solution chemistry, the proposed mechanistic pathways for the reaction of 2-propanol on H-ZSM-5 are given below:

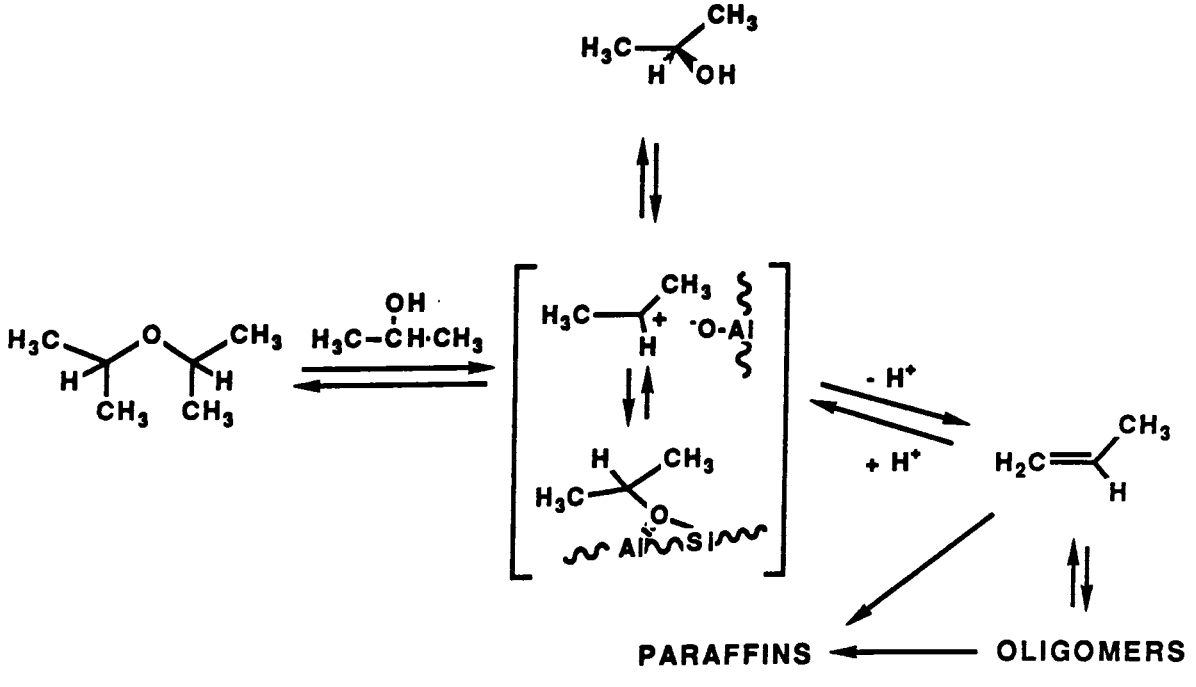

When the alcohol comes in contact with the acid site, the alcohol may be protonated, and a molecule of water expelled forming a carbenium ion or an alkoxide with the lattice. If both

these intermediates exist, it is likely that they are in equilibrium with each other. One of the initial goals of this project was to observe the reactive intermediate to help elucidate the total reaction mechanism. If a molecule of 2-propanol collides with the intermediate, diisopropyl ether may be formed. Since the formation of the ether involves collision with the reactive intermediate, any condition that improves the stability of the intermediate, increases its lifetime, or increases it concentration should increase the yield of diisopropyl ether. The intermediate may also lose a proton to form propene. Propene may then desorb and leave the system or collide with other intermediates which would lead to oligomerization. The oligomers may then disproportionate and form paraffins and alkenes.

While the search for direct spectroscopic proof of the intermediate(s) was not successful, several other important mechanistic details were revealed. It was determined that the intermediate does not go through a cyclopropyl carbenium ion intermediate, the build up of oligomer is necessary before significant production of propene occurs and once the oligomer is formed it does not exchange with any of the incoming alcohol molecules. These results and the experiments that prove them will be discussed in detail.

2-Propanol on H-ZSM-5 in a non-flowing system.

In the initial batch experiment the temperature was increased from room temperature up to 180°C and the resulting spectra monitored. At room temperature there were two obvious peaks, (Figure 3.1) a large broad peak at approximately 63 ppm and a small resonance at approximately 19 ppm. The large resonance is from the labelled number 2 carbon on the alcohol which has a chemical shift of 63.4 relative to TMS in solution.(*38*) The absolute shift of the alcohol is not known because an internal standard was not used but many molecules adsorbed on zeolites do not shift significantly from their solution values. The small peak is from an aliphatic carbon, which implies that even at room temperature there is some hydrocarbon formation. The small peak is not due to the one and three positions of the alcohol because the chemical shift of these carbons is about 25 ppm. Also the one and three

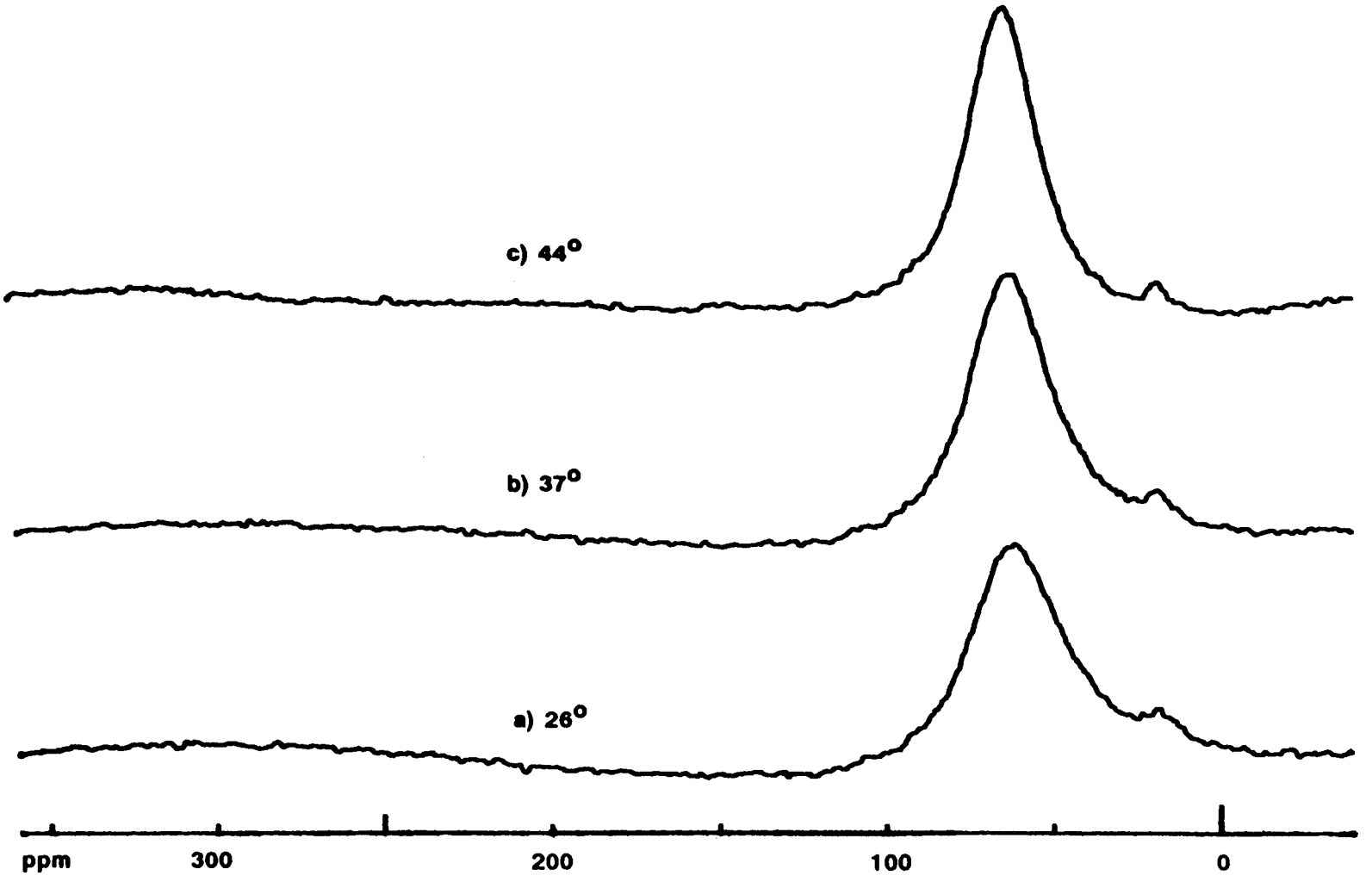

Figure 3.1 ^{13}C spectra of 2-propanol on H-ZSM-5 in a non-flowing system. a) 0-10 min. b) 22-32 min. c) 44-54 min.

carbons are not labelled and would not be in high enough concentration to be seen. At low temperature the adsorbed species have limited mobility so the peaks are very broad (1400 and 250 Hz respectively). These peaks are so broad that they may be obscuring signals from similar species. As the temperature increases, the alcohol peak narrows to less than 700 Hz (Figure 3.2). This narrowing can be attributed to greater mobility of the alcohol on the catalyst. At 90° C and approximately 5 hours after heating was begun, a spectrum of 30,000 scans was taken to check for low concentration species (Figure 3.3). This spectrum revealed no apparent changes so the temperature was increased. Approximately 45 minutes after the temperature reached 110° C, a small broad peak could be seen in the aliphatic region (Figure 3.4). There is also a very broad region slightly downfield from 100 ppm which may be due to adsorbed propene or higher alkenes. During the next 50 minutes at 110° C the 2-propanol peak disappeared and the aliphatic region continued to grow as the propene oligomerized (Figure 3.5). The very broad resonance around 100 ppm also disappears which would add credence to the resonance being from alkenes. The aliphatic peak is about 1500 Hz wide. The aliphatic peak is broad for two reasons: the polymerized product has limited mobility and a wide variety of methyl, methylene and methine carbons in a variety of environments can be formed by hydride and methyl shifts on the oligomer chain. At 110° C a spectrum of 1,000 scans was taken with a pulse delay of 250 ms but it appeared identical to the other spectra (Figure 3.6). The temperature was increased to 180° C over the next 90 minutes. As the temperature increased, the aliphatic peak began to resolve into three main resonances at 24, 17, and 7 ppm (Figure 3.7, 3.8). This triad looks similar to polymeric hydrocarbon spectra, such as polypropylene, but the shifts are slightly upfield from comparable solution spectra. As the temperature approaches 180°, the peak farthest downfield appears to be increasing in intensity. This increase may be due to increased mobility of one type of carbon or at the higher temperature the oligomer may undergo more skeletal rearrangements. The skeletal rearrangements (Figure 3.9) may be linearizing the branched chain because in the next spectrum (Figure 3.10), when the flow of nitrogen gas is started, this resonance decreases and a linear hydrocarbon would desorb more readily then a branched hydrocarbon. The

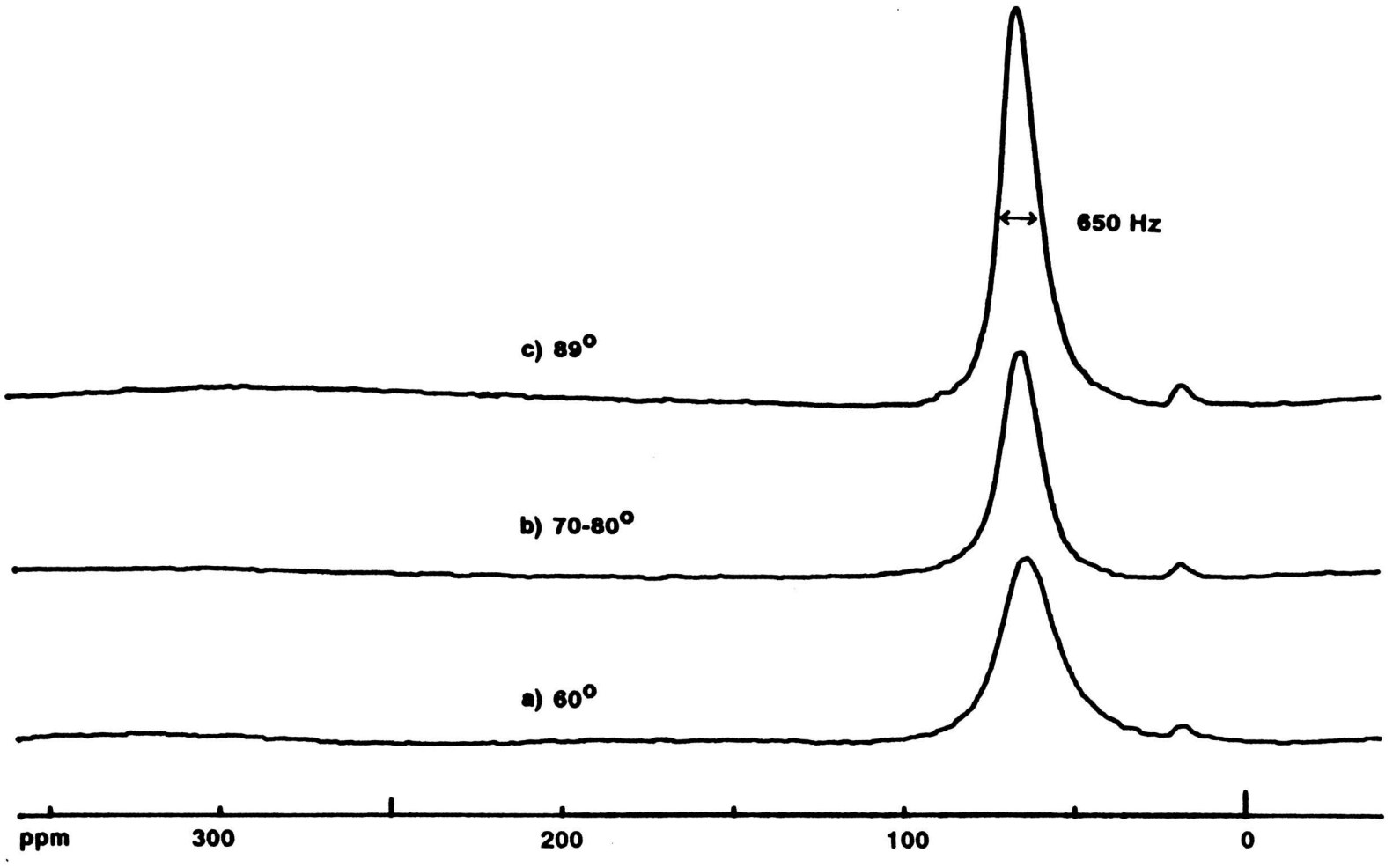

Figure 3.2 ^{13}C spectra of 2-propanol on H-ZSM-5 in a non-flowing system. a) 66-76 min. b) 88-98 min. c) 312-322 min.

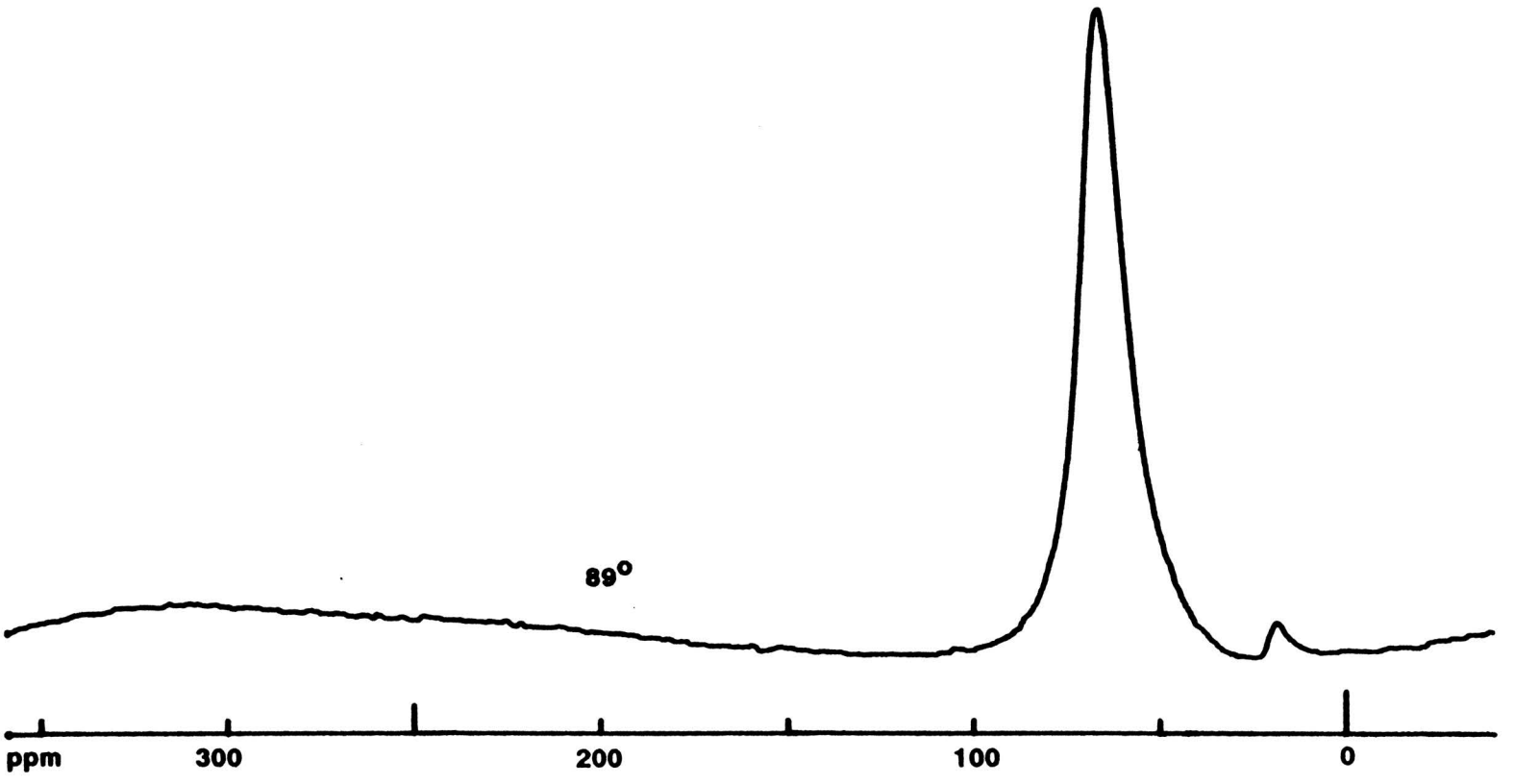

Figure 3.3 ^{13}C spectrum of 2-propanol on H-ZSM-5 in a non-flowing system. 30,000 scans, 323-353 min.

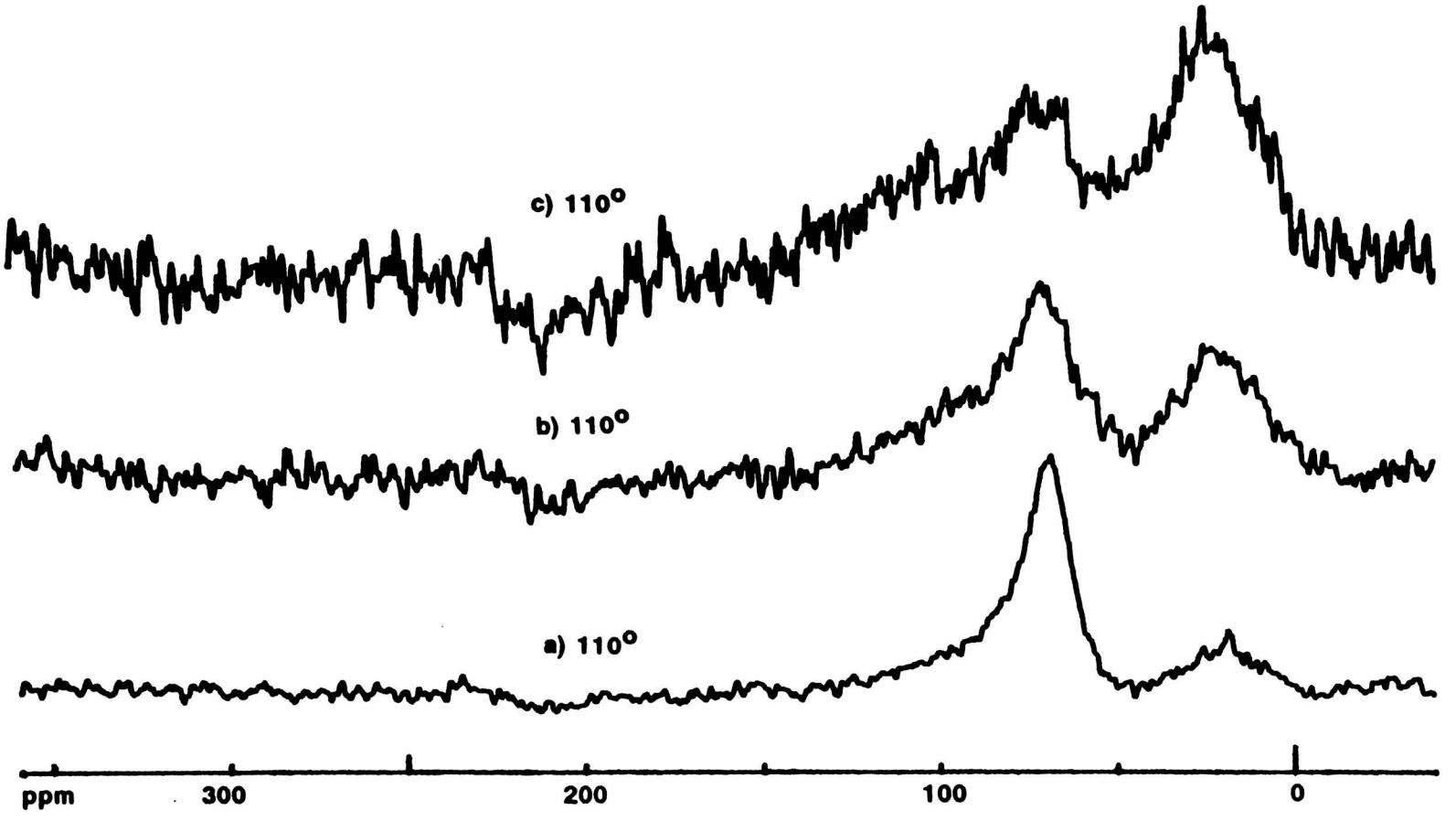

Figure 3.4 ^{13}C spectra of 2-propanol on H-ZSM-5 in a non-flowing system. a) 510-520 min. b) 521-531 min. c) 535-545 min.

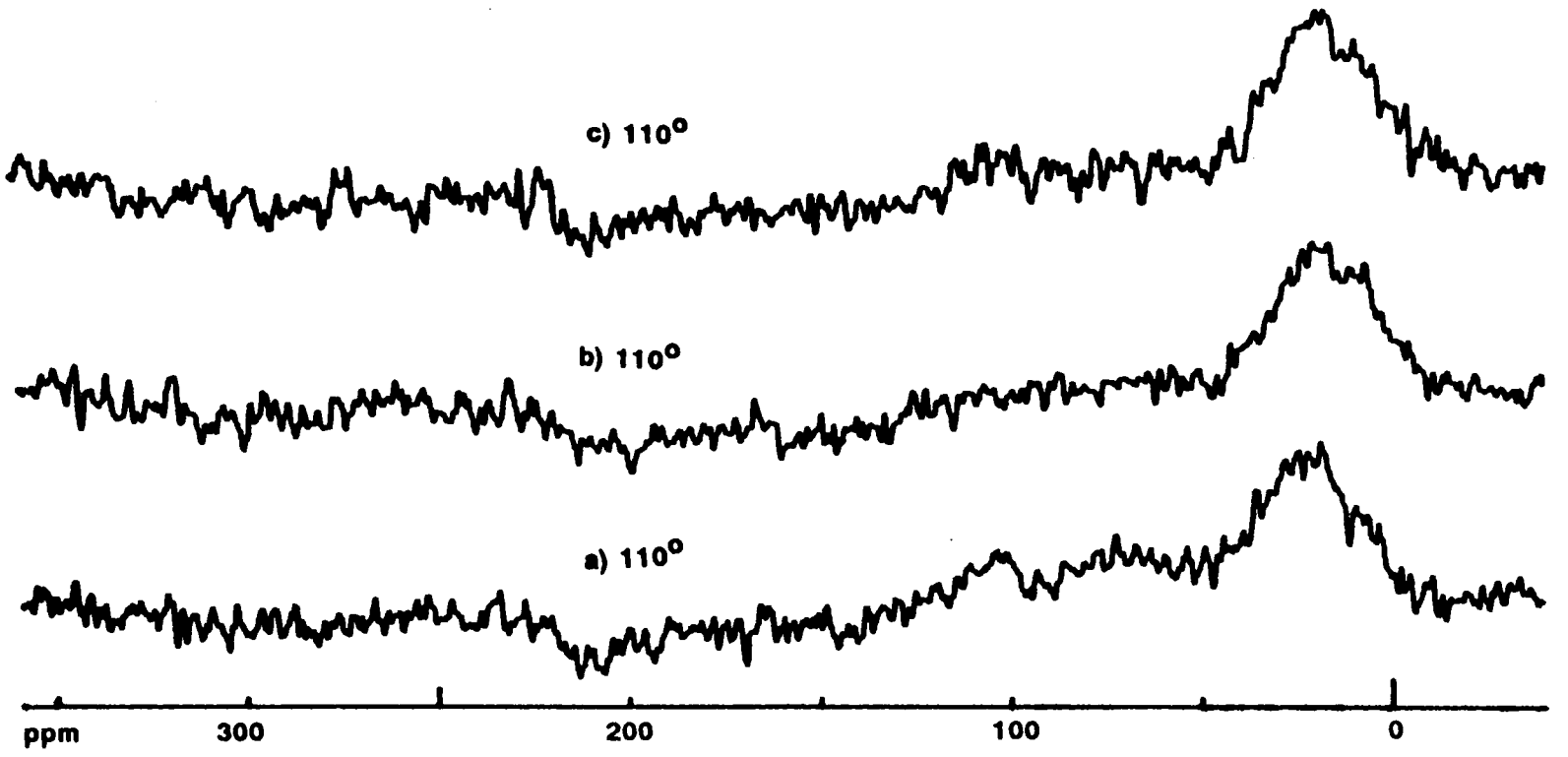

Figure 3.5 ^{13}C spectra of 2-propanol on H-ZSM-5 in a non-flowing system. a) 547-557 min. b) 560-570 min. c) 573-583 min.

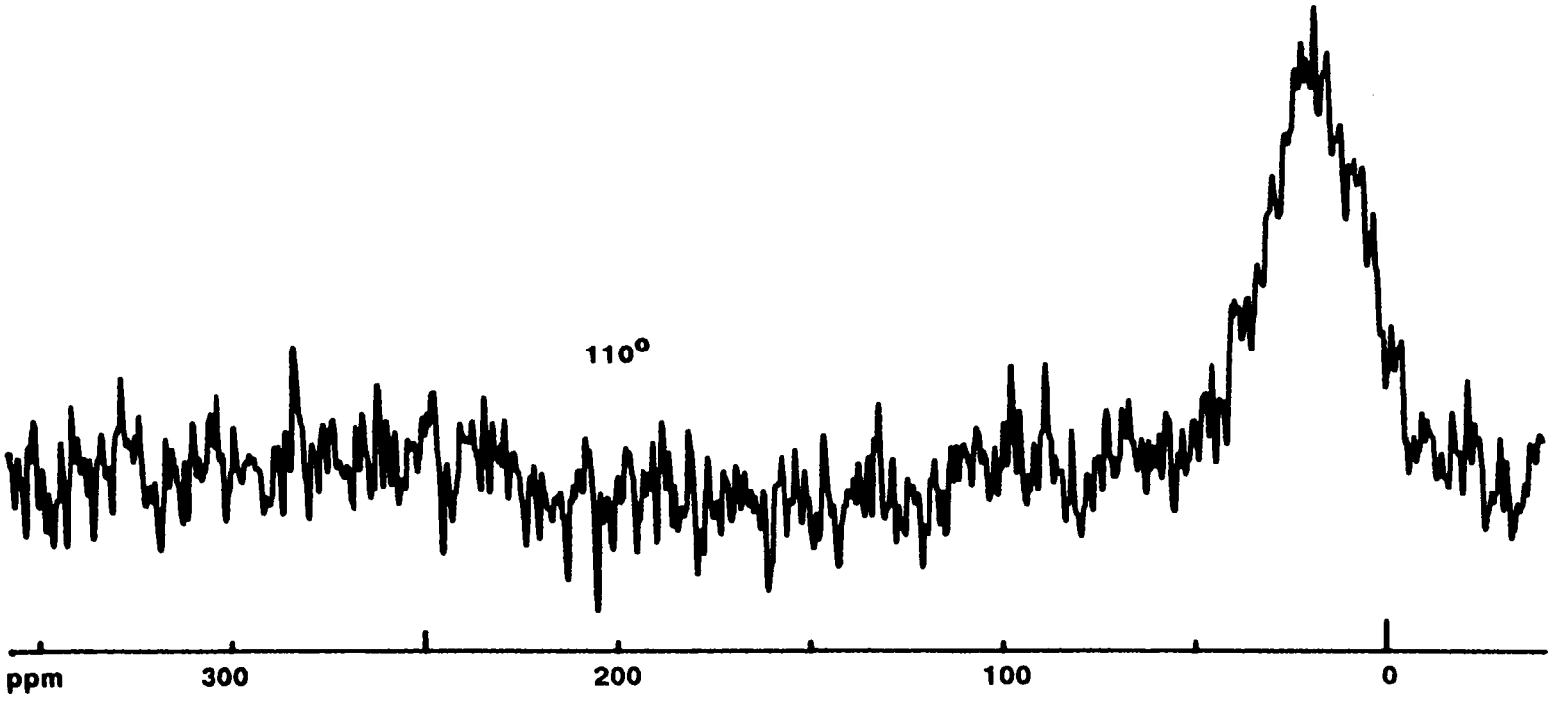

Figure 3.6 ^{13}C spectrum of 2-propanol on H-ZSM-5 in a non-flowing system. 1,000 scans with a pulse delay of 250 ms. 596-606 min.

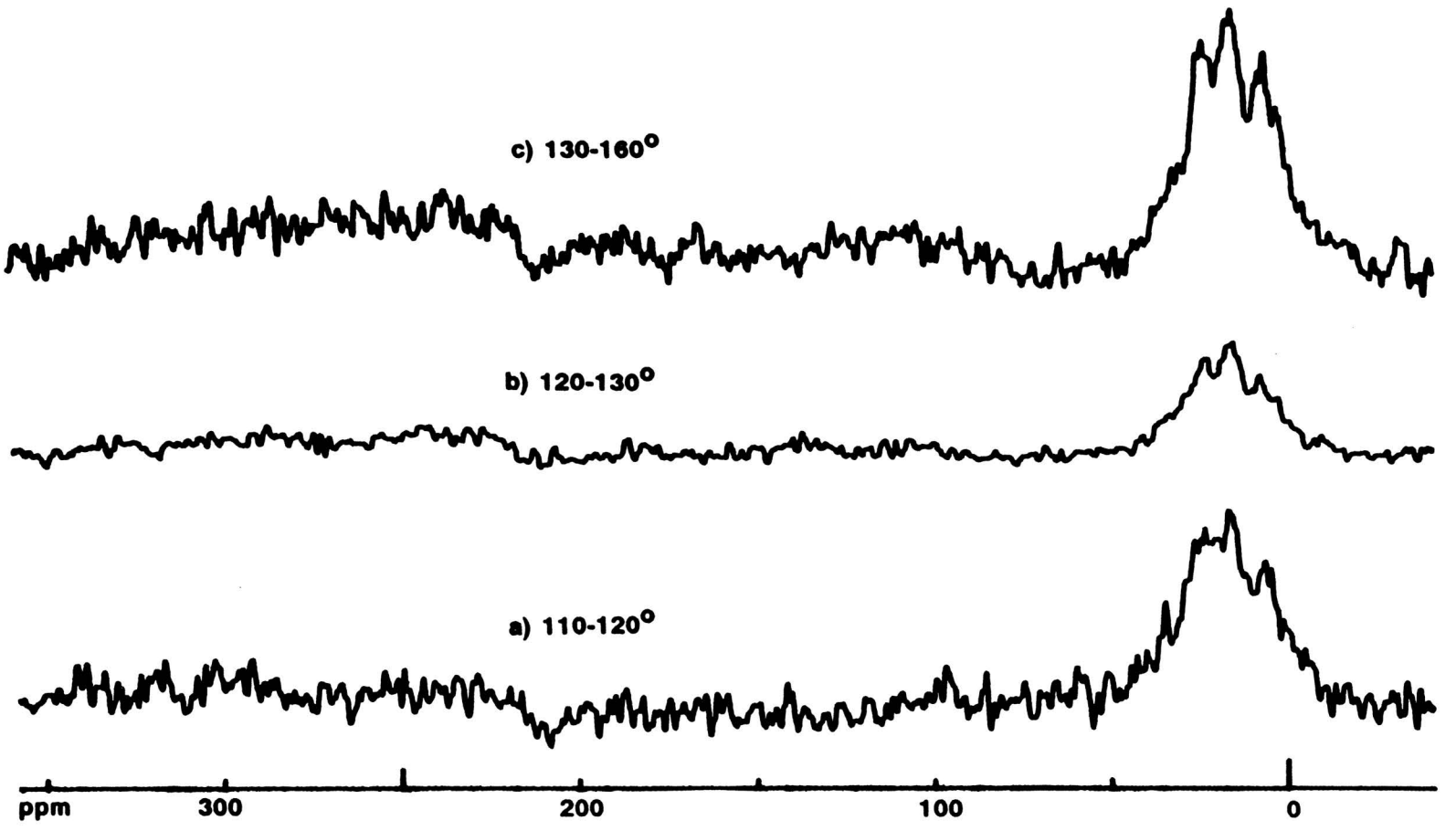

Figure 3.7 ^{13}C spectra of 2-propanol on H-ZSM-5 in a non-flowing system. a) 610-620 min. b) 637-647 min. c) 664-674 min.

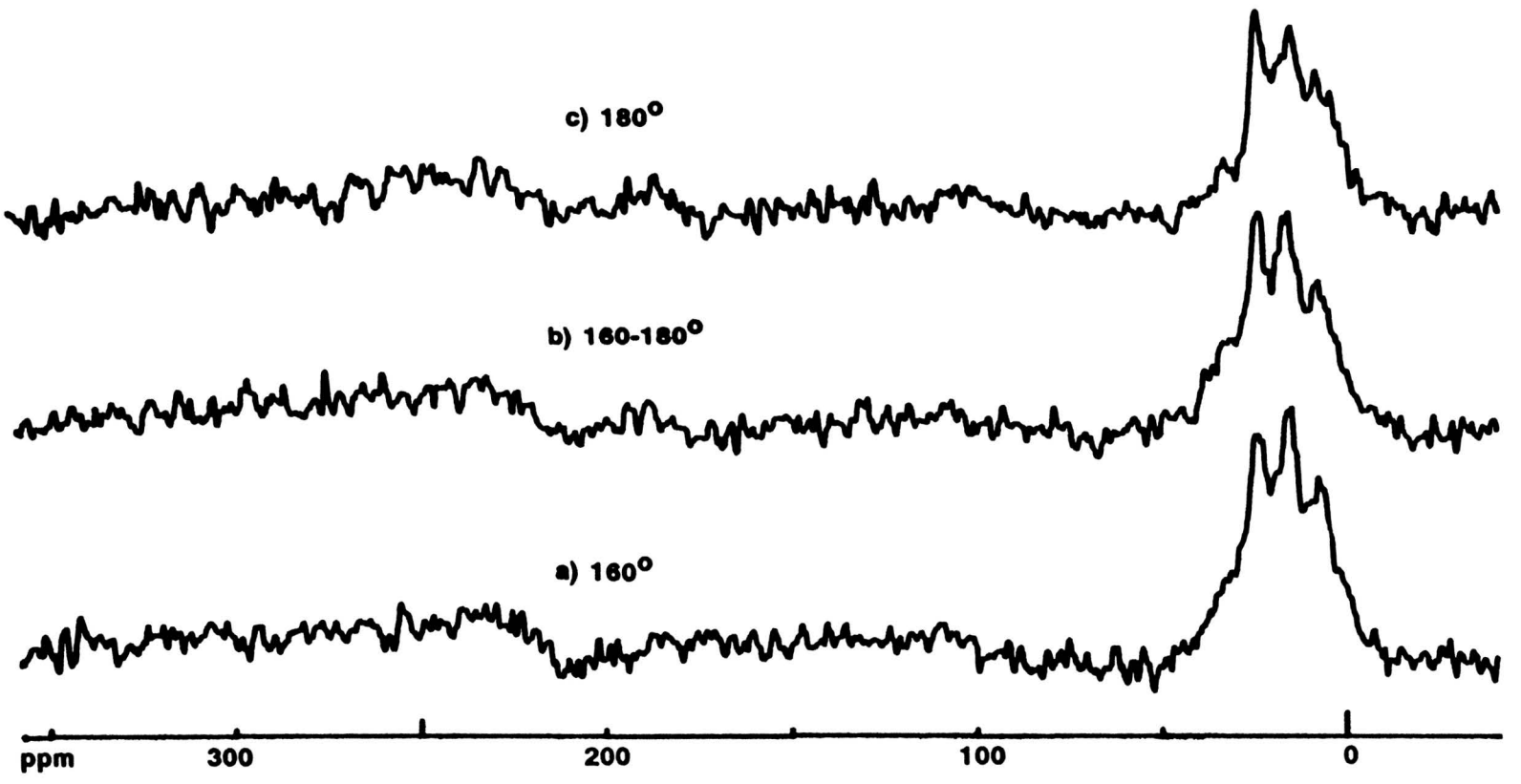

Figure 3.8 ^{13}C spectra of 2-propanol on H-ZSM-5 in a non-flowing system. a) 680-690 min. b) 692-702 min. c) 704-714 min.

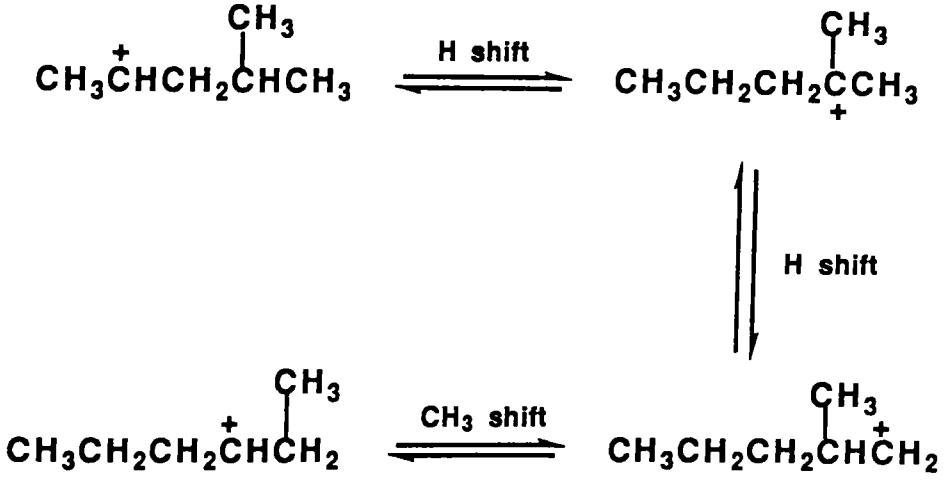

Figure 3.9 Possible mechanism of branched hydrocarbon linearization.

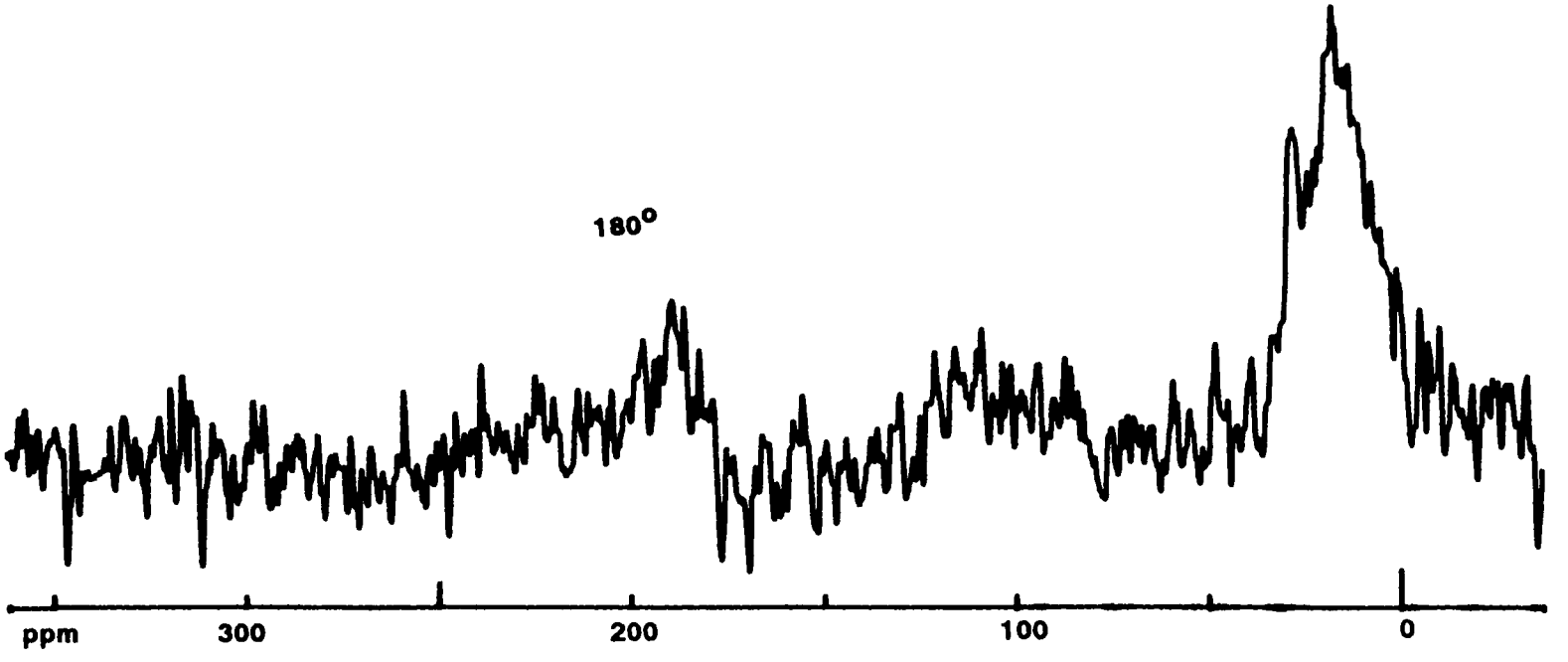

Figure 3.10 ^{13}C spectrum of 2-propanol on H-ZSM-5 in a non-flowing system after flow of nitrogen gas was started. 754-764 min.

formation of branched isomers is thermodynamically favored over the formation of linear isomers but since the linear molecules may desorb more readily, the equilibrium may be shifted in their favor. The linearization process may be similar to the isomerization of xylene over H-ZSM-5. When the xylene is in the pores of the zeolite it undergoes various rearrangements and several species may exist in the pores but the product is virtually only p-xylene because p-xylene diffuses out of the pores over one thousand times faster than the meta isomer.(*41*)

2-Propanol flowing over H-ZSM-5 between 100 and 130° C

The second set of experiments was one of the most enlightening because we used a flowing stream and the products were collected and monitored by high resolution ^{13}C NMR. From the previous trials it appeared that most of the interesting chemistry began at over 100° C so the second trial began by flowing 2-propanol over the catalyst that was already equilibrated to 100°. In the first ten minute block, the 2-propanol was easily visible (Figure 3.11). The next ten minute block revealed a large alcohol peak and a small resonance at approximately 19 ppm. Both of these peaks appeared to be due to only one species. After almost two hours at 100° the flow spectra remained invariant and no products were found in the Br_2/CCl_4 trap (Figure 3.12). The temperature was increased to 110° and held for one hour. During this time the flow spectra did not change but the Br_2/CCl_4 trap showed the presence of diisopropyl ether, 2-propanol, 1,2-dibromopropane and 2-bromopropane. It was anticipated that at the lower temperatures the H-ZSM-5 would produce diisopropyl ether. The 2-propanol probably comes from incomplete conversion on the catalyst, the 1,2-dibromopropane is the expected resultant of the brominated propene and the 2-bromopropane is generated in the trap from either the nucleophilic substitution of the alcohol or the Markovnikov addition of HBr to the alkene. The identities of the peaks were confirmed by spiking the sample with known compounds. The second product spectra collected at 110° showed an increase in the products collected (Figure 3.13). When the temperature was

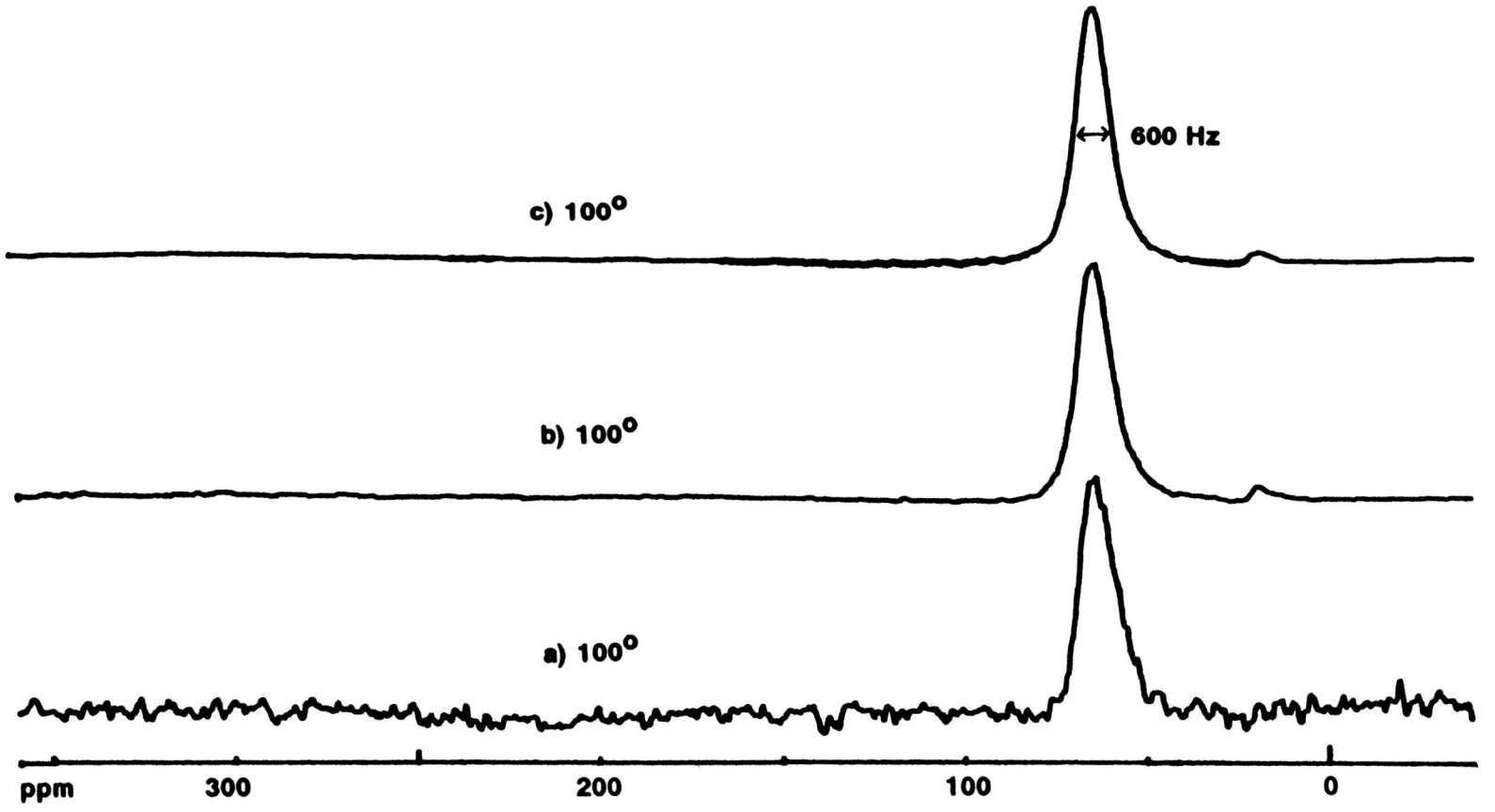

Figure 3.11 ^{13}C spectra of 2-propanol flowing over H-ZSM-5. a) 0-10 min. b) 11-21 min. c) 22-32 min.

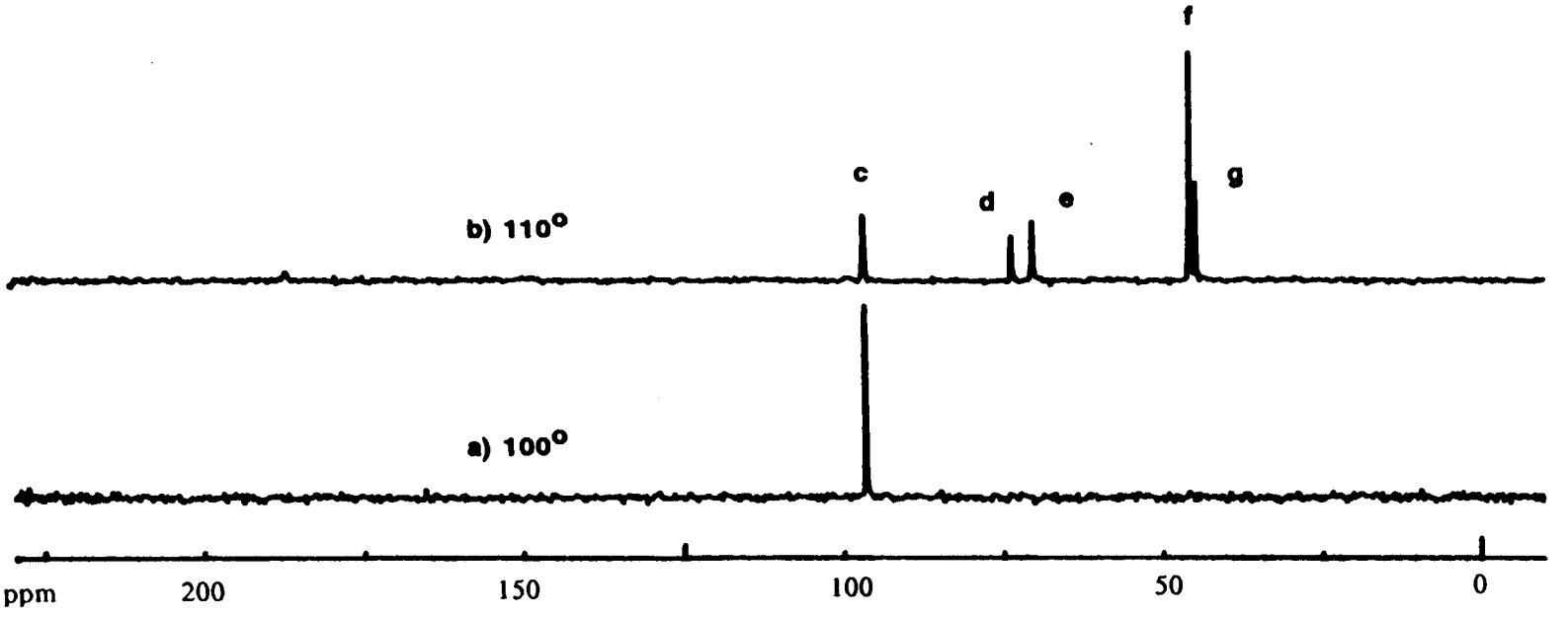

Figure 3.12 High resolution ^{13}C spectra of the collected products from flowing 2-propanol over H-ZSM-5. a) 21-51 min. b) 111-141 min.

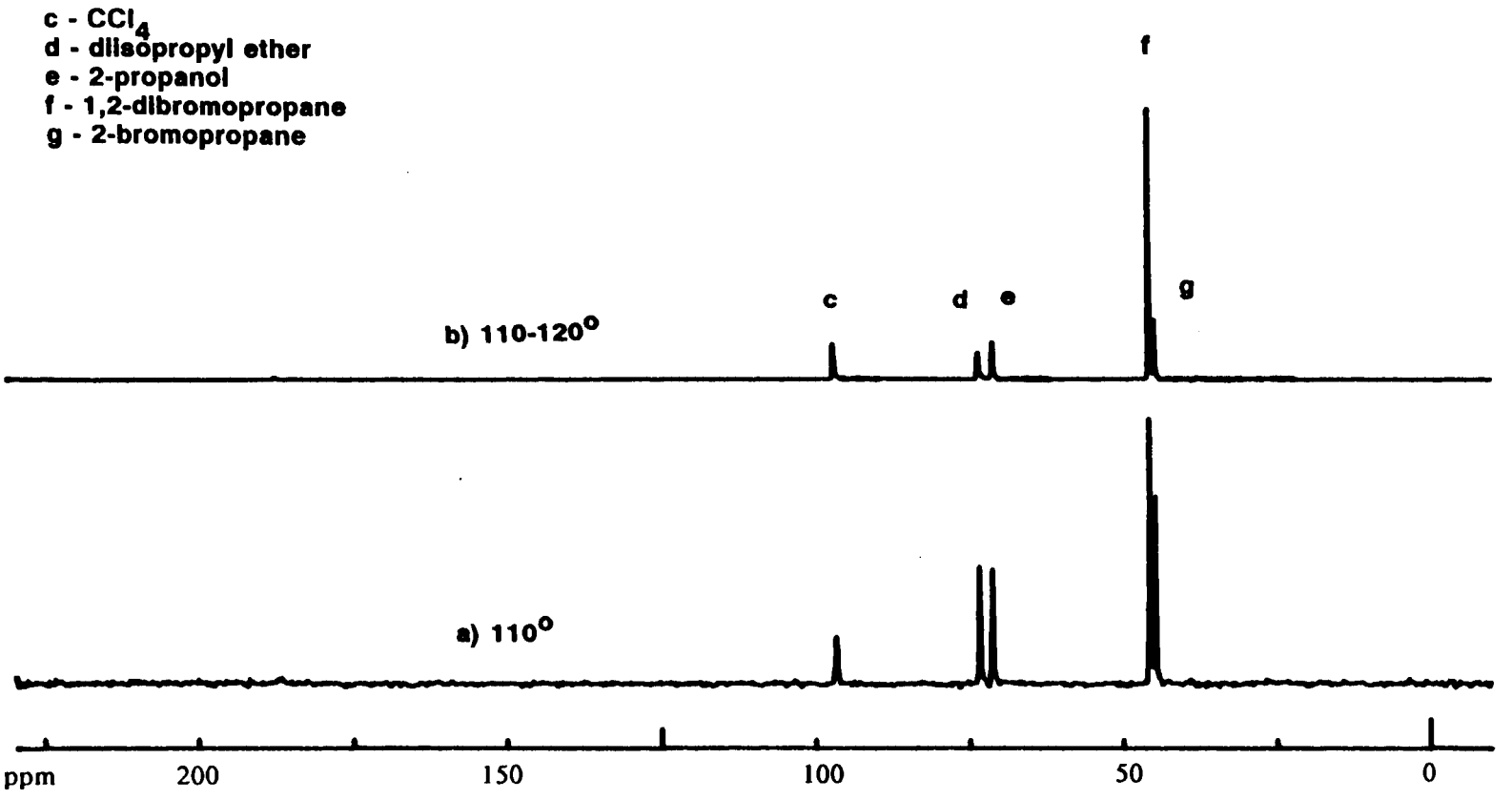

Figure 3.13 High resolution ^{13}C spectra of the collected products from flowing 2-propanol over H-ZSM-5. a) 141-171 min. b) 171-201 min.

increased to 110°-120° the relative amount of propene in the product stream greatly increased.

An important question that must be addressed is: why did we see collected products, but not any spectroscopic evidence of their formation on the catalyst? There are two plausible explanations for the lack of signal on the flow NMR. First, the concentration of the reaction centers is not very high and once the products are formed, those that desorb will be gases. Since gases have relatively long T_1 relaxation times, their signal will quickly become saturated in our system with the short (12 ms) pulse delays and pass through the catalyst undetected.

The flow system was held at 120° C for half and hour, with no noticeable differences in the flow spectra. During this time, the collected product showed no diisopropyl ether and an increase in the amount of propene (Figure 3.14). The formation of diisopropyl ether occurs from the collision of a 2-propanol molecule with the reactive intermediate. The disappearance of the ether probably implies that the intermediate has a shorter lifetime at the higher temperature, so it forms propene before it collides with another molecule of 2-propanol. A second less likely explanation is that the diisopropyl ether is formed but the ether is cleaved at another acid site. When the catalyst temperature is increased to 130° C, the aliphatic region rapidly grows at the expense of the alcohol peak (Figure 3.15). The aliphatic peak grows until it is approximately 1500 Hz wide (Figure 3.16) and as on the previous trial, there appear to be three main types of carbon. On some of the spectra, each of the three main peaks appear to be split into doublets. This shift difference may be due to the oligomer residing in different environments in the catalyst (i.e. one in the elliptical channels and one in the circular channels) As soon as the aliphatic region began to grow on the flow NMR, the propene was totally consumed in the formation of the oligomer and no products were present in the product stream (Figure 3.14). After about 90 minutes at 130° the relative intensity of the alcohol to the aliphatic region remained constant (Figure 3.17). Once this "steady-state" was achieved the product stream contained essentially only propene (Figure 3.18). The disappearance and reemergence of the propene may be explained by the increased reactivity of the intermediate at 130°. At 130° propene is formed rapidly, but before it can exit the catalyst, it contacts another reactive intermediate and oligomerizes. As

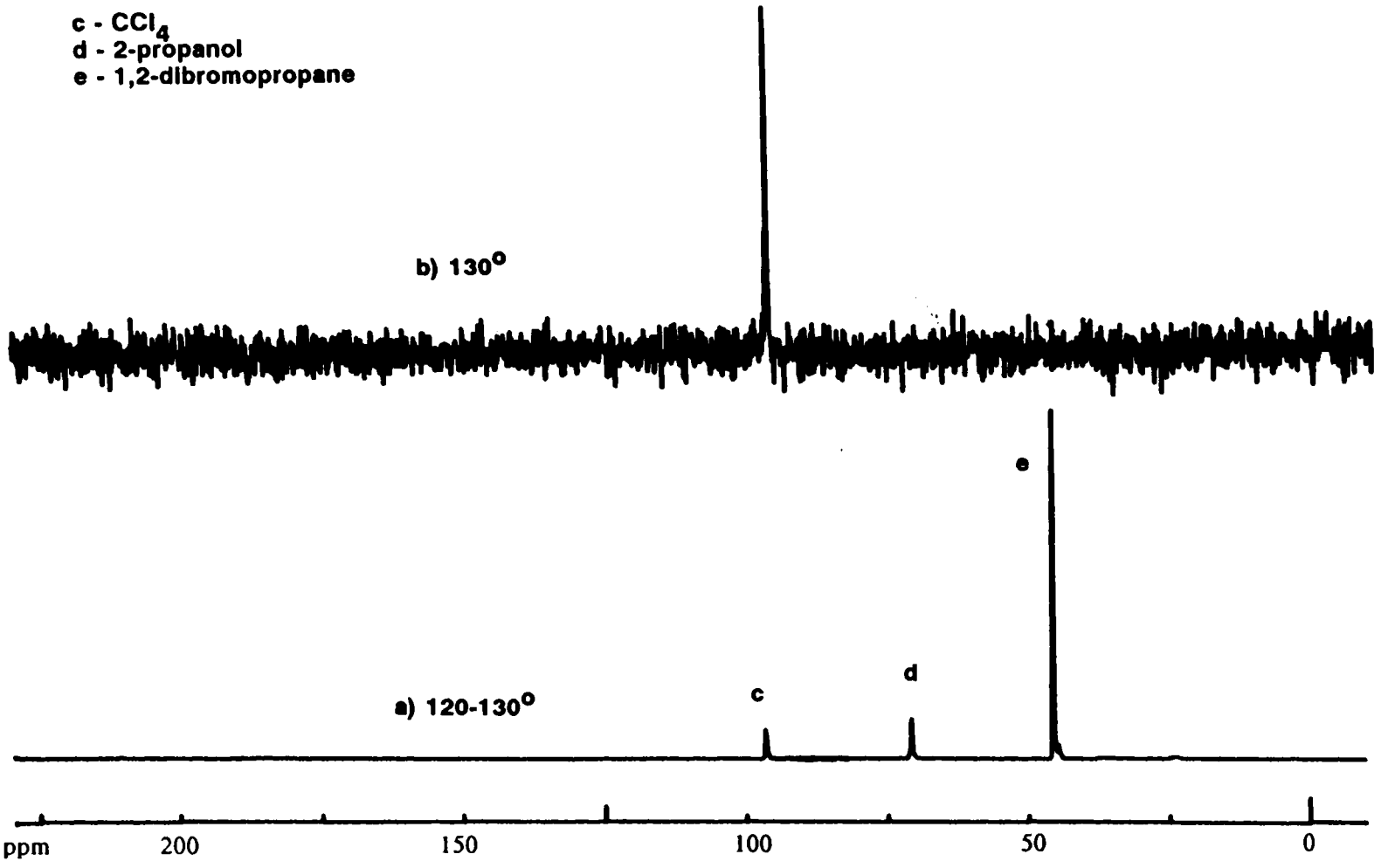

Figure 3.14 High resolution ^{13}C spectra of the collected products from flowing 2-propanol over H-ZSM-5. a) 201-231 min. b) 261-291 min.

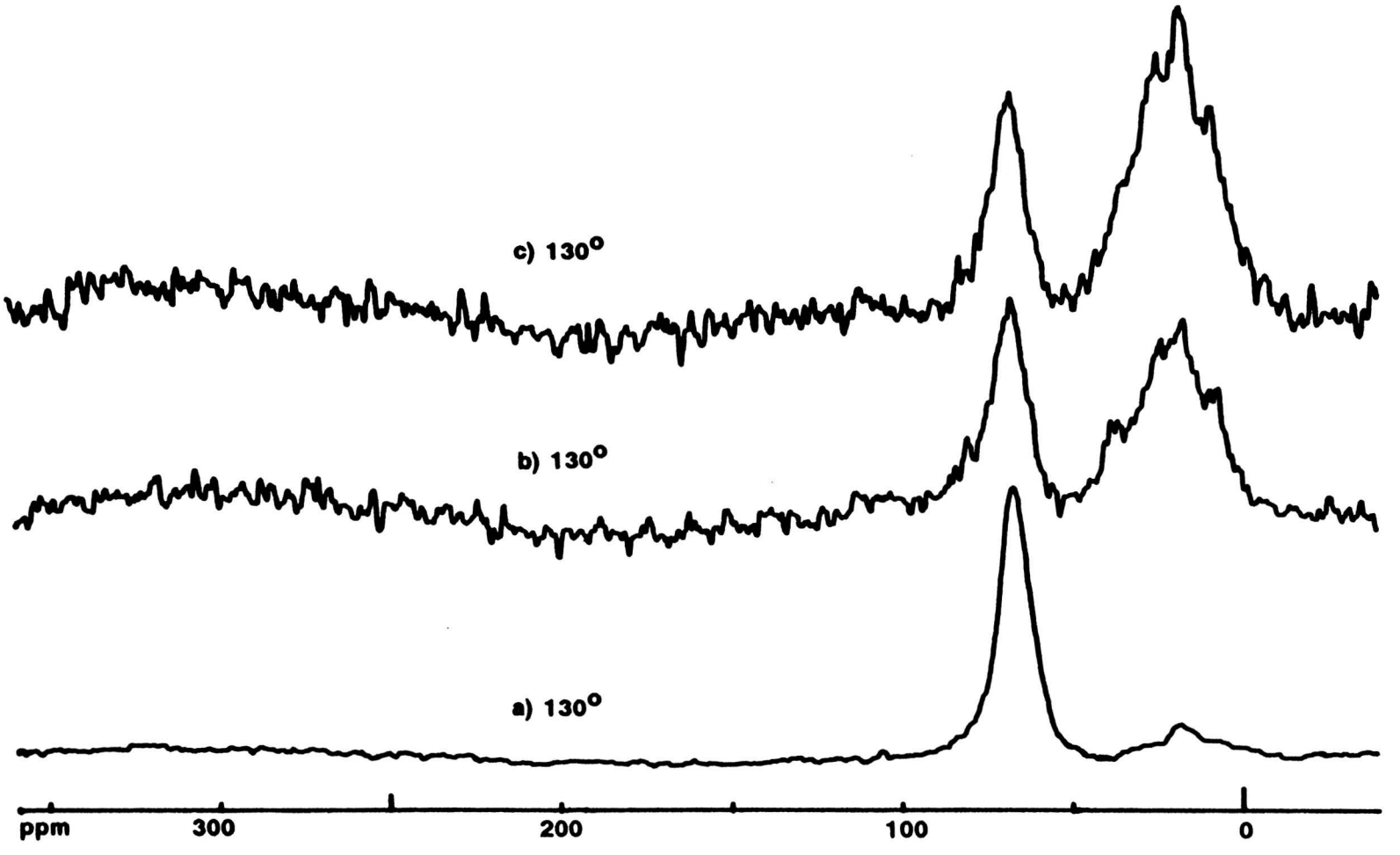

Figure 3.15 ^{13}C spectra of 2-propanol flowing over H-ZSM-5. a) 229-239 min. b) 240-250 min. c) 251-261 min.

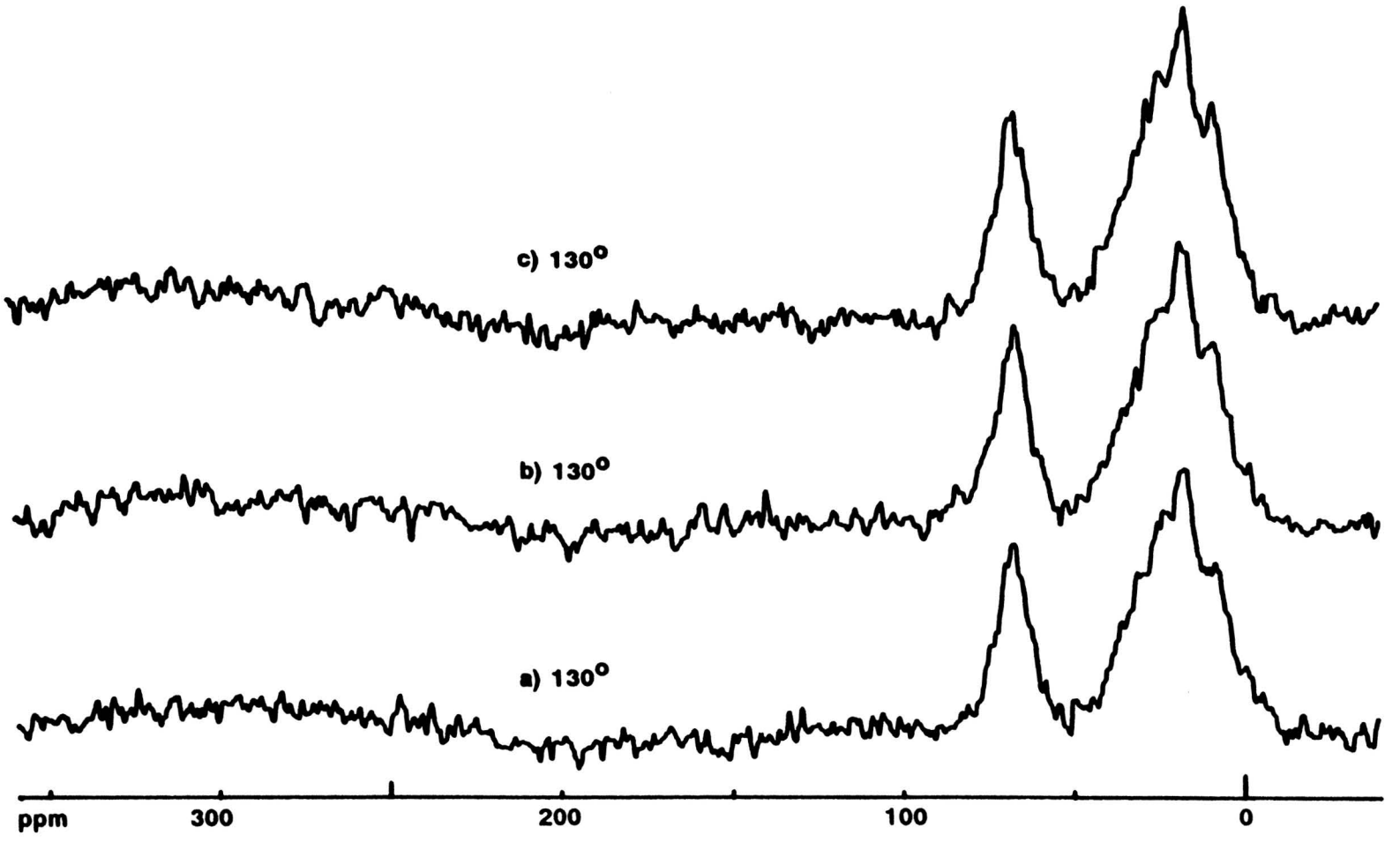

Figure 3.16 ^{13}C spectra of 2-propanol flowing over H-ZSM-5. a) 262-272 min. b) 273-283 min. c) 284-294 min.

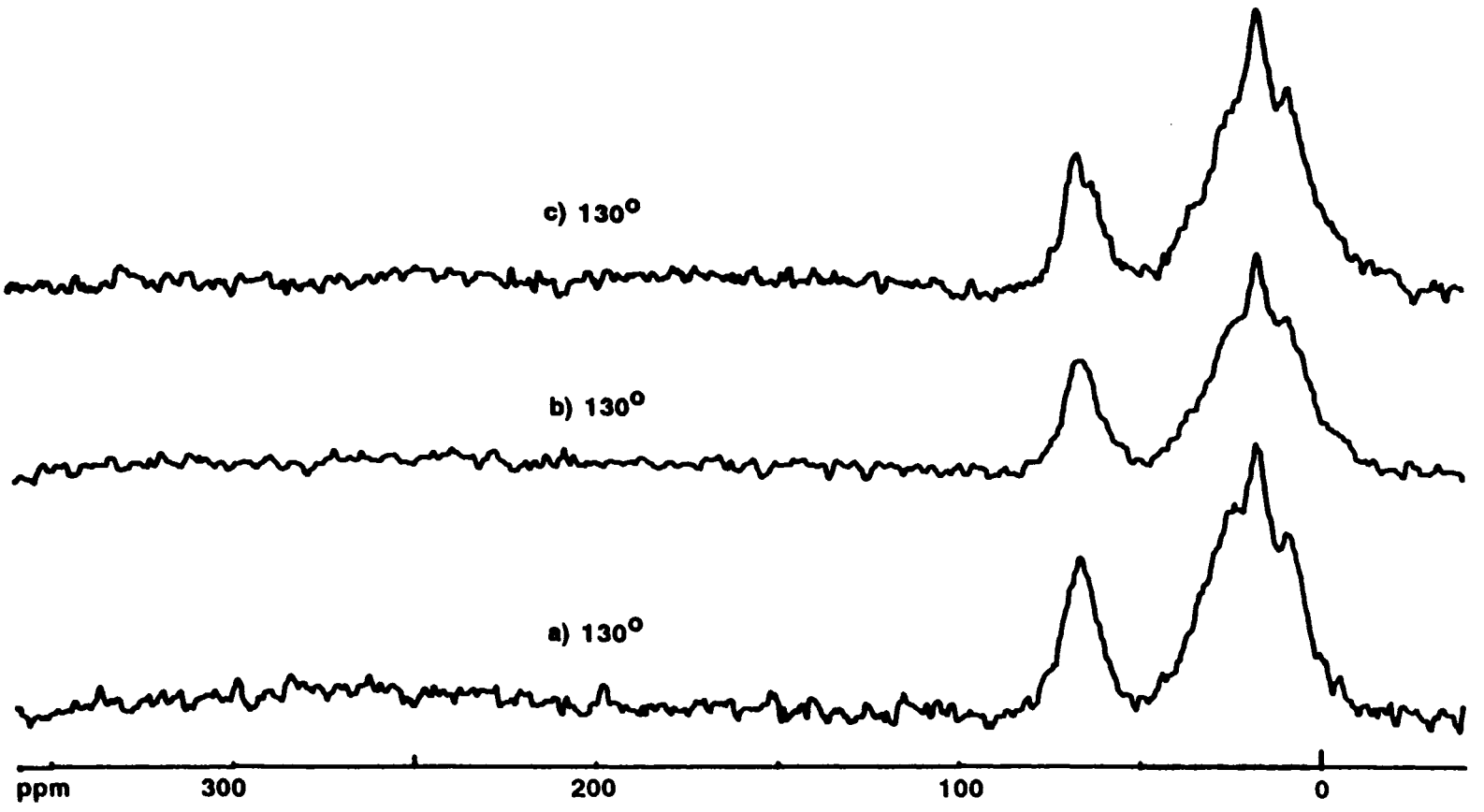

Figure 3.17 ^{13}C spectra of 2-propanol flowing over H-ZSM-5. a) 319-329 min. b) 330-340 min. c) 341-351 min.

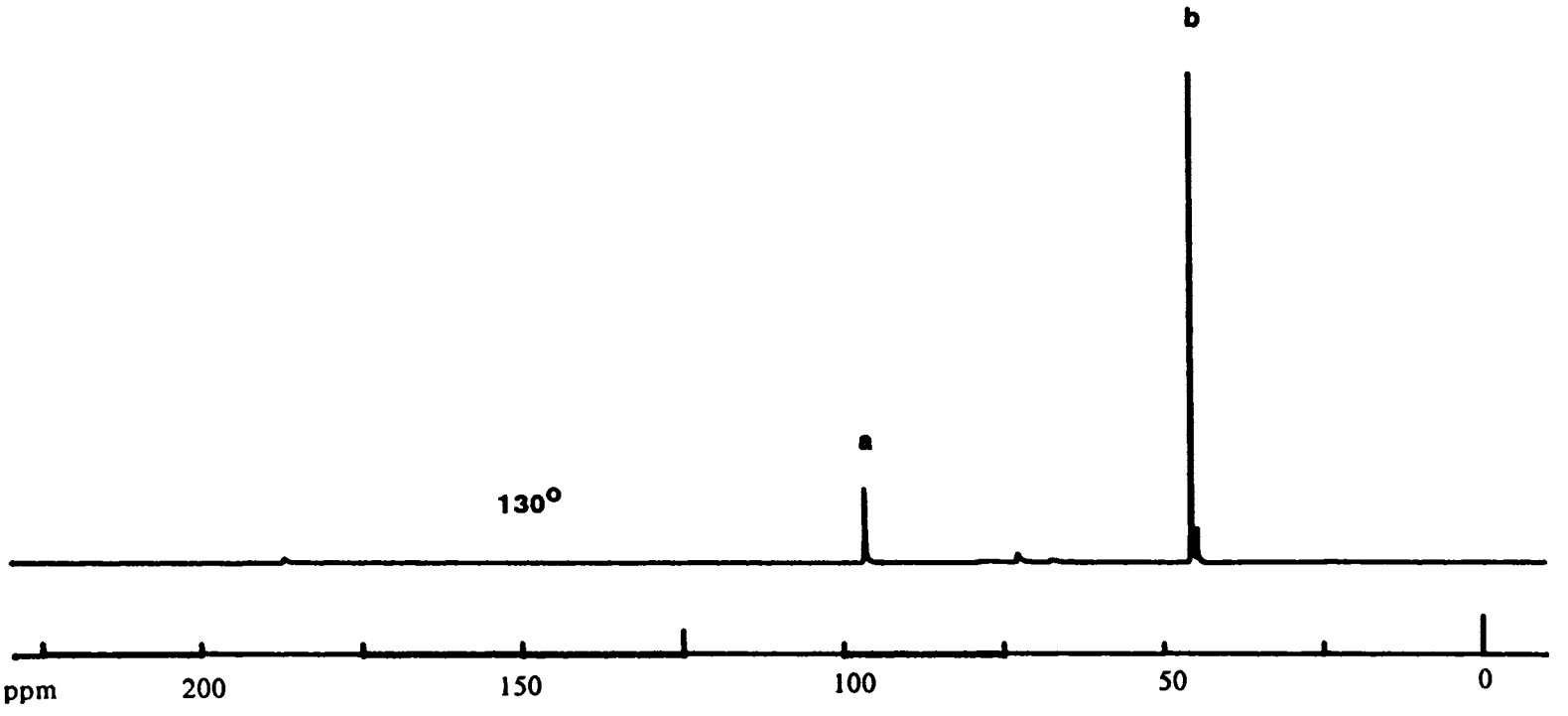

Figure 3.18 High resolution ^{13}C spectrum of the collected products from flowing 2-propanol over H-ZSM-5. 321-419 min.

the oligomers grow they slowly fill up the channels and decrease the availability of active sites, so the newly formed propene may exit the system before colliding with another reactive site. The nature of the acid site may also change during oligomer formation. As the channels become more crowded the ability of a planar carbenium ion to exist may decrease. If the reactive intermediate is a carbenium ion there is the possibility of the of the label rearranging by formation of a cyclopropyl carbenium ion. Figure 3.19 illustrates how the formation of a cyclopropyl carbenium ion would scramble the label. To disprove the cyclopropyl carbenium ion hypothesis the ^{13}C spectra of the 1,2-dibromopropane was expanded. (Figure 3.20) The one and three carbons should produce 3 peaks each. A central resonance flanked by two identical peaks due to splitting from the adjacent ^{13}C. The ratio of these peaks were in the same isotopic ratio as the starting material. The cyclopropyl rearrangement may not occur because once a carbenium ion is formed it loses a proton or collides with another molecule faster than it can rearrange. Alternatively, the carbenium ion may be strongly associated with the lattice oxygen so that it behaves more like an alkoxide which would not be able to rearrange.

Approximately two and a half hours after reaching 130° the nitrogen flow bypassed the alcohol bubbler. The alcohol peak disappeared within 10 minutes (Figure 3.21) and the remaining aliphatic region did not noticeably change during the remaining 45 minutes of the experiment (Figure 3.22). The product stream did not include any aliphatic desorption products after the flow of 2-propanol was diverted.

The used catalyst was a light tan and TGA and DTA were performed on the catalyst by the Chemical Engineering Department. The sample lost approximately 5% by weight between 275 and 375° C which is characteristic of hydrocarbon type residues. If a density for liquid hydrocarbons is assumed, the 5% weight loss corresponds to about one-third of the void space being filled if one assumes all of the residue to be within the crystal.(*1*)

Although the spectra from this experiment turned out nicely we still did not observe a carbenium ion or alkoxide type intermediate. If our system had one intermediate per aluminum atom the concentration should have been sufficient for detection, particularly when

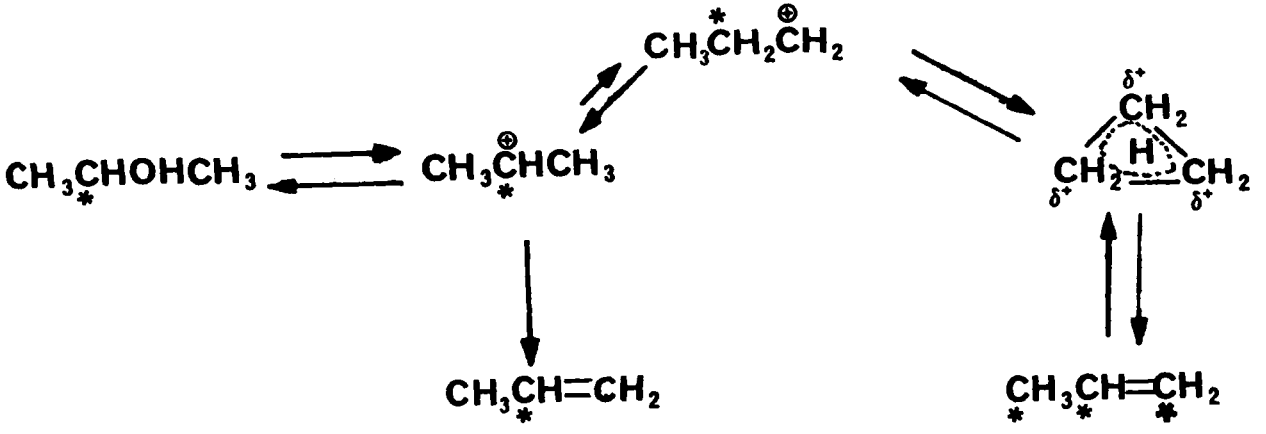

Figure 3.19 Mechanism of label scrambling via a cyclopropyl carbenium ion.

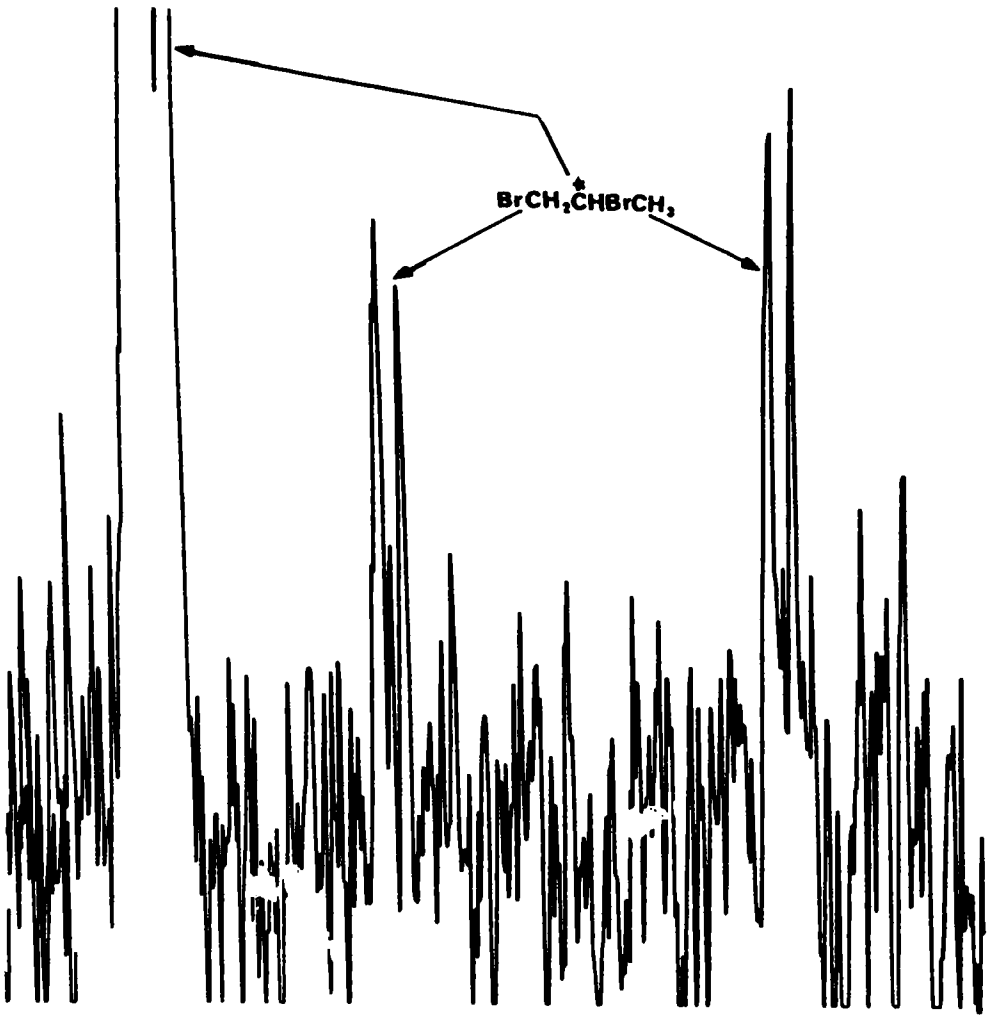

Figure 3.20 Expanded high resolution ^{13}C spectrum of 1,2-dibromopropane from product trap.

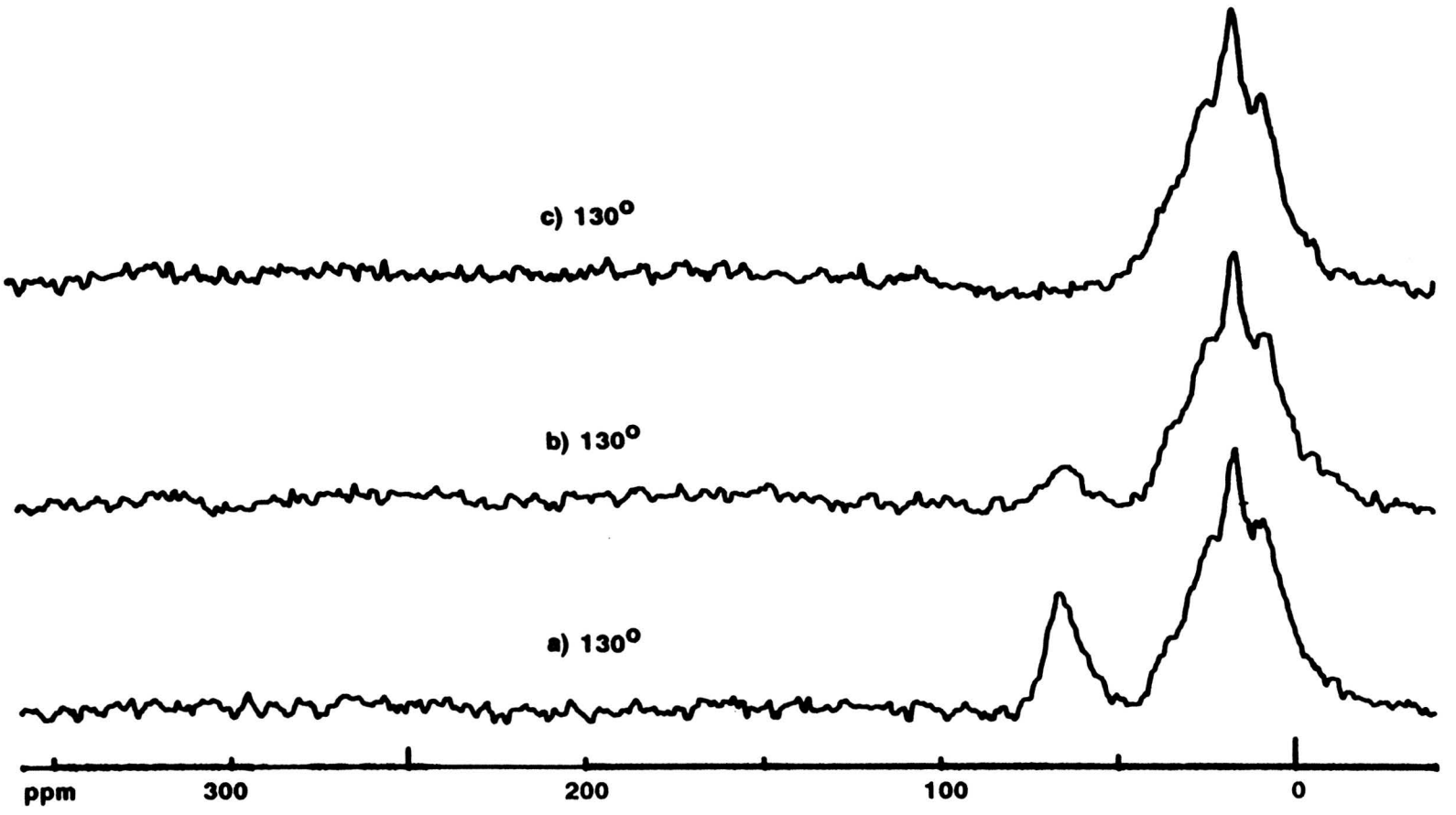

Figure 3.21 ^{13}C spectra of 2-propanol flowing over H-ZSM-5. a) 363-373 min. b) Flow to 2-propanol bypassed, 375-385. c) 386-396 min.

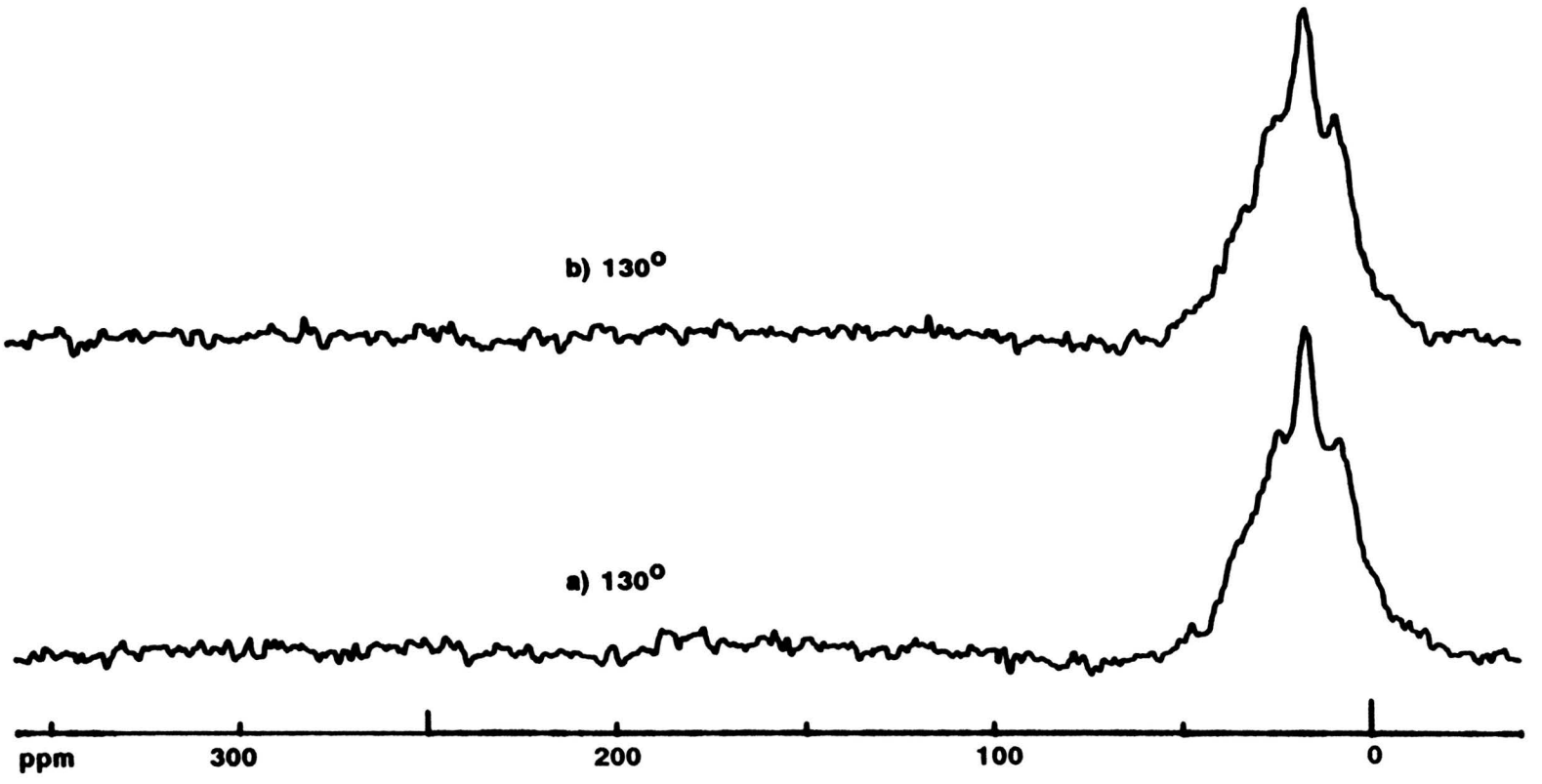

Figure 3.22 ^{13}C spectra of 2-propanol flowing over H-ZSM-5 after flow to the alcohol has been bypassed. a) 398-408 min. b) 409-419 min.

the system was scanned for half an hour. The only way we would not see the intermediates were if they did not exist or if they reacted or exchanged quickly within the NMR time frame. The most likely explanation is the latter. If the carbenium ion is in rapid equilibrium with an alkoxide to the lattice the chemical shift would be the weighted average of the two species. Since an alkoxide would be expected around 75 ppm and secondary carbocation around 300 ppm the signal from an exchanging species would be so broad that it would be below our limits of detection.

2-Propanol flowing over H-ZSM-5 at 180° C

This experiment was similar to the previous one except that the temperature remained at 180°. The first ten minute spectrum is very noisy, but two broad resonances are discernable (Figure 3.23). One peak is centered just over 100 ppm and the other is in the aliphatic region. In the aliphatic region there is one sharp peak about 17 ppm. Since there is no shift standard, this can not be unambigously identified but it does imply that initially the label has not rearranged into a variety of carbon types. The broad resonance above 100 ppm may be due to a variety of alkenes. Oligomer formation is significant in the second spectrum and the broad resonance around 100 ppm has almost disappeared. During the first hour, the aliphatic resonance continued to grow and the peak width (about 1500 Hz) and shape were similar to the run at 130° (Figure 3.24). It appears that the oligomerization process occurs at both temperatures only at different rates. The higher rate of conversion at 180° is evidenced by the fact that we never see an alcohol resonance at 180°. None of the traps had any products until the one collected between 42 and 100 minutes (Figure 3.25). Although this represents a longer collection time than most of the other traps, the concentration of the desorbed products was fairly low. The collected products were all in the aliphatic region and they appeared to be mainly hexane and 2-methylpentane. After about one hour a block of 1,000 scans with a pulse delay of one second was taken to check for species with longer T_1's (Figure 3.26). The longer pulse delay barely changed the spectrum and no other species were

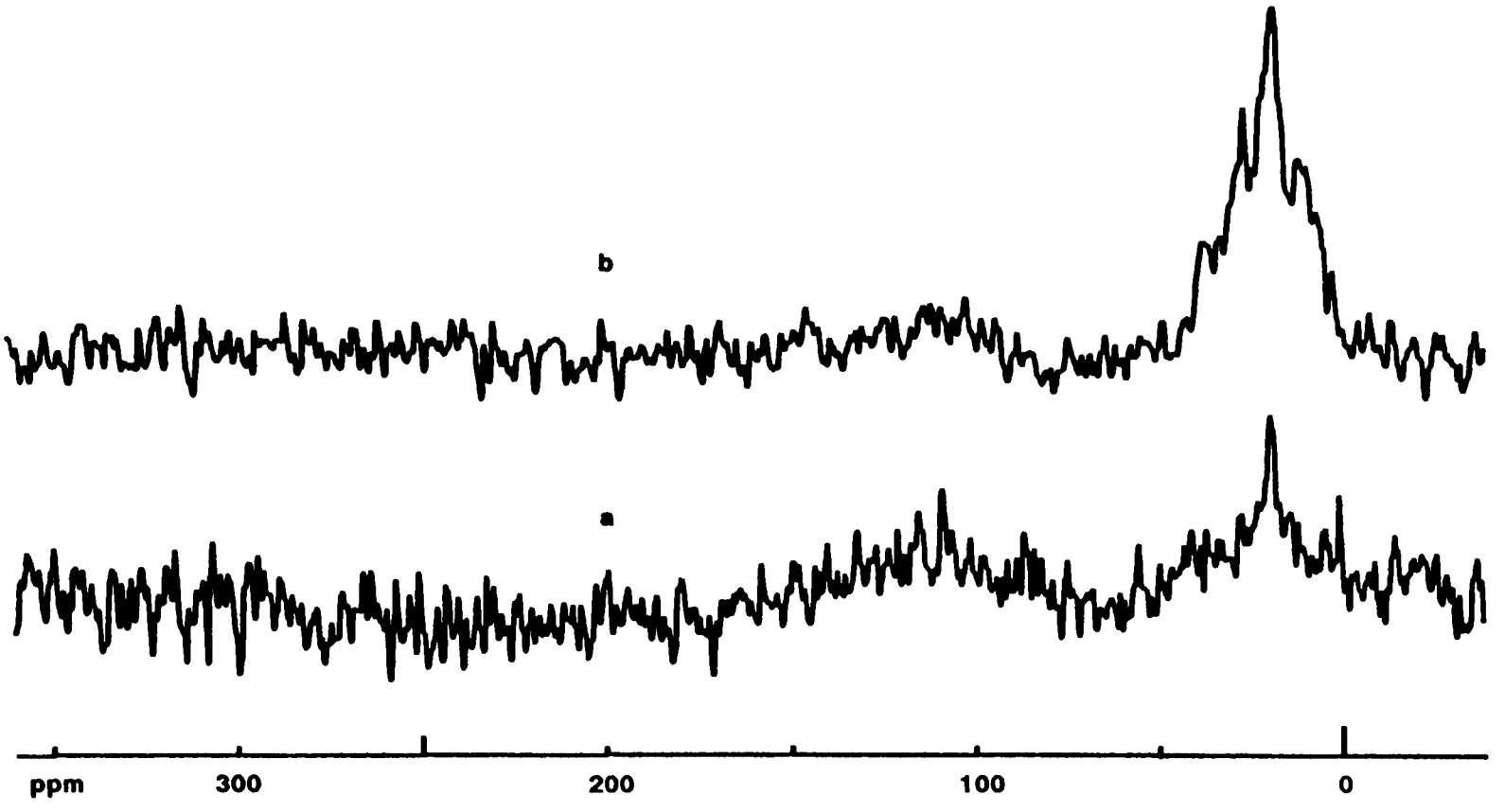

Figure 3.23 ^{13}C spectra of 2-propanol flowing over H-ZSM-5 at 180°. a) 0-10 min. b) 11-21 min.

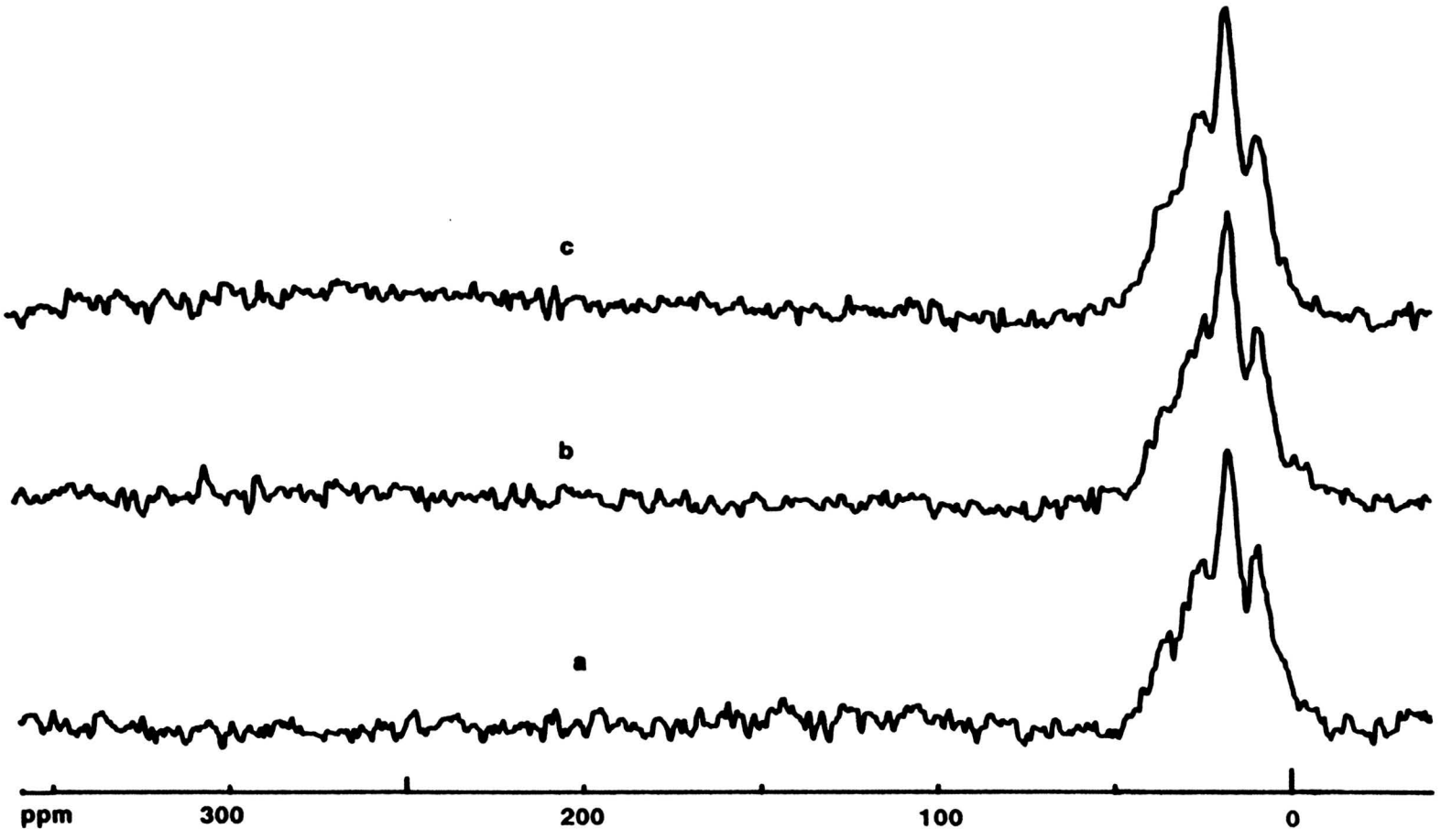

Figure 3.24 ^{13}C spectra of 2-propanol flowing over H-ZSM-5 at 180^{o}. a) 21-31 min. b) 32-42 min. c) 43-53 min.

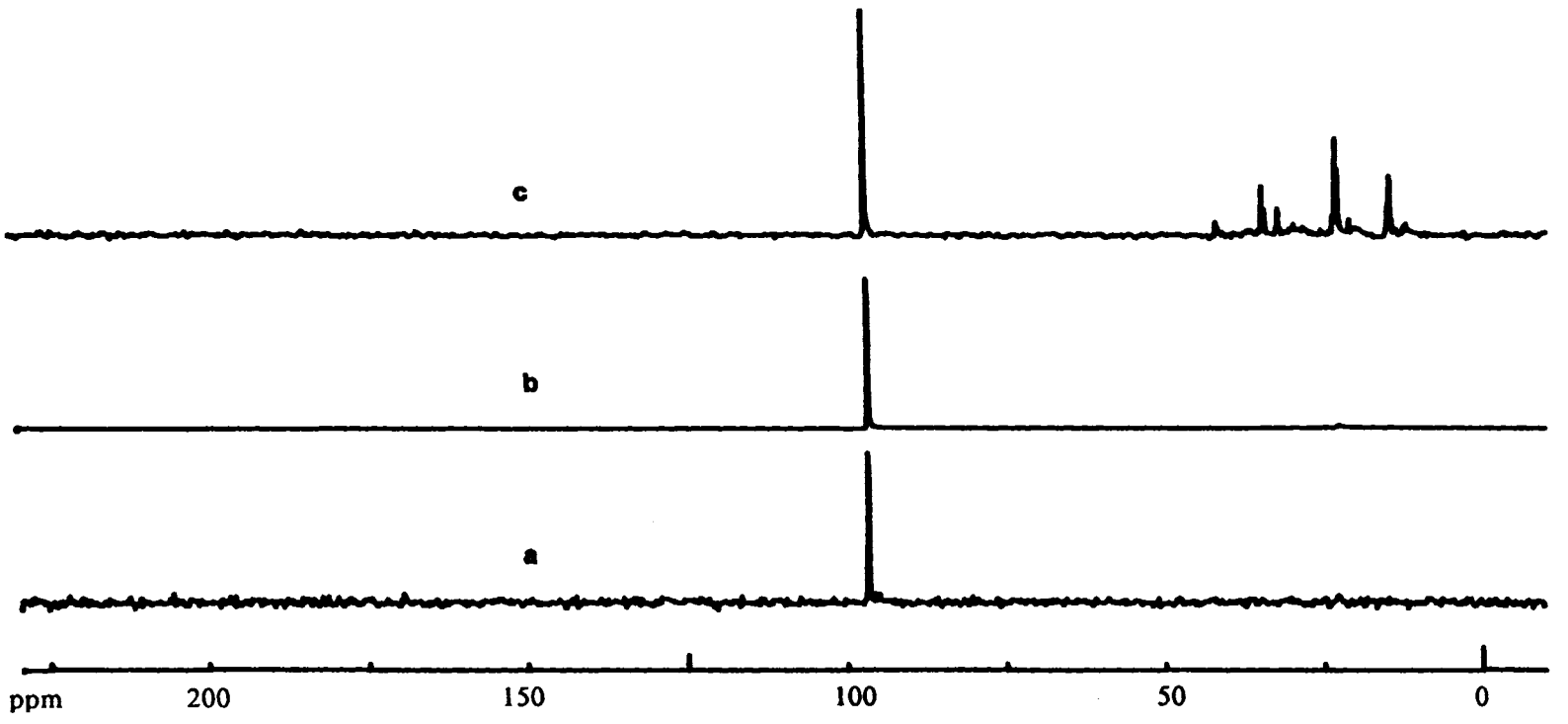

Figure 3.25 High resolution ^{13}C spectra of the collected products from 2-propanol flowing over H-ZSM-5 at 180°. a) 0-11 min. b) 31-42 min. c) 42-100 min.

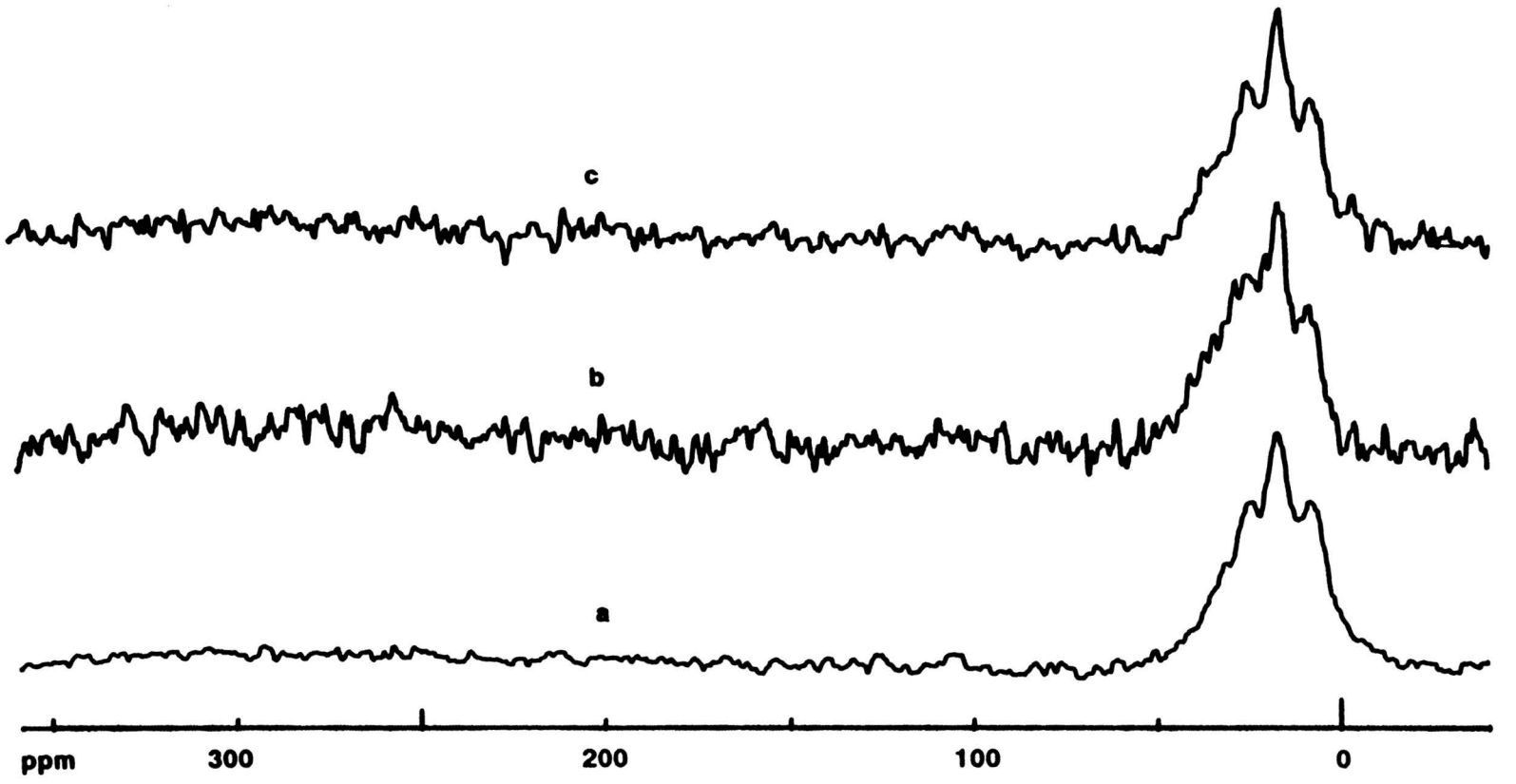

Figure 3.26 ^{13}C spectra of 2-propanol flowing over H-ZSM-5 at 180°. a) 1,000 scans with a pulse delay of 1 second; 66-88 min. b) 2,000 scans; 102-104 min. c) 3,000 scans; 115-118 min.

observed.

In an attempt to see an alcohol peak, the flow was diverted from the bubbler, the bubbler warmed, opened to the system for 30 seconds, then bypassed again. No 2-propanol signal was seen in the 2,000 scan spectrum. This was repeated a second time only the alcohol was flowed for three minutes and this also produced no changes in the spectrum. After two hours the 2-propanol was bypassed and several spectra run (Figure 3.27). The oligomerized region changed very little during this time.

The used catalyst was a light tan so it was analyzed by solid-state NMR. Solid-state NMR was necessary because we did not know if our flow system was capable of seeing species of limited mobility. The results of the solid-state experiment, both with and without cross polarization, were very satisfying because they were identical to our flow results except the solid-state experiment had better resolution and higher signal to noise (Figure 3.28). It should also be noted that there were no peaks in the alkene region which confirms the absence of olefins.

Flowing labelled 2-propanol followed by non-labelled 2-propanol over H-ZSM-5 at 130°

One of the drawbacks of the previous experiments was that we could not accurately measure the water coming off the catalyst and we could not get immediate feedback when the products were only collected in solution. The use of gas chromatography solved this problem. During the optimization of the chromatography several experiments were run at 130° using non-labelled 2-propanol. The chromatography showed several interesting trends. The only product observed for approximately the first two hours was water. The water was liberated from the reaction of the alcohol at the acid site. With the first sign of propene, the amount of water decreased and went to a steady value as the propene quickly increased and then reached a steady state. On some trials, after the propene had polymerized and deactivated a portion of the catalyst, some 2-propanol was seen in the product stream. The most interesting phenomenon occurred when the flow to the alcohol was bypassed and then

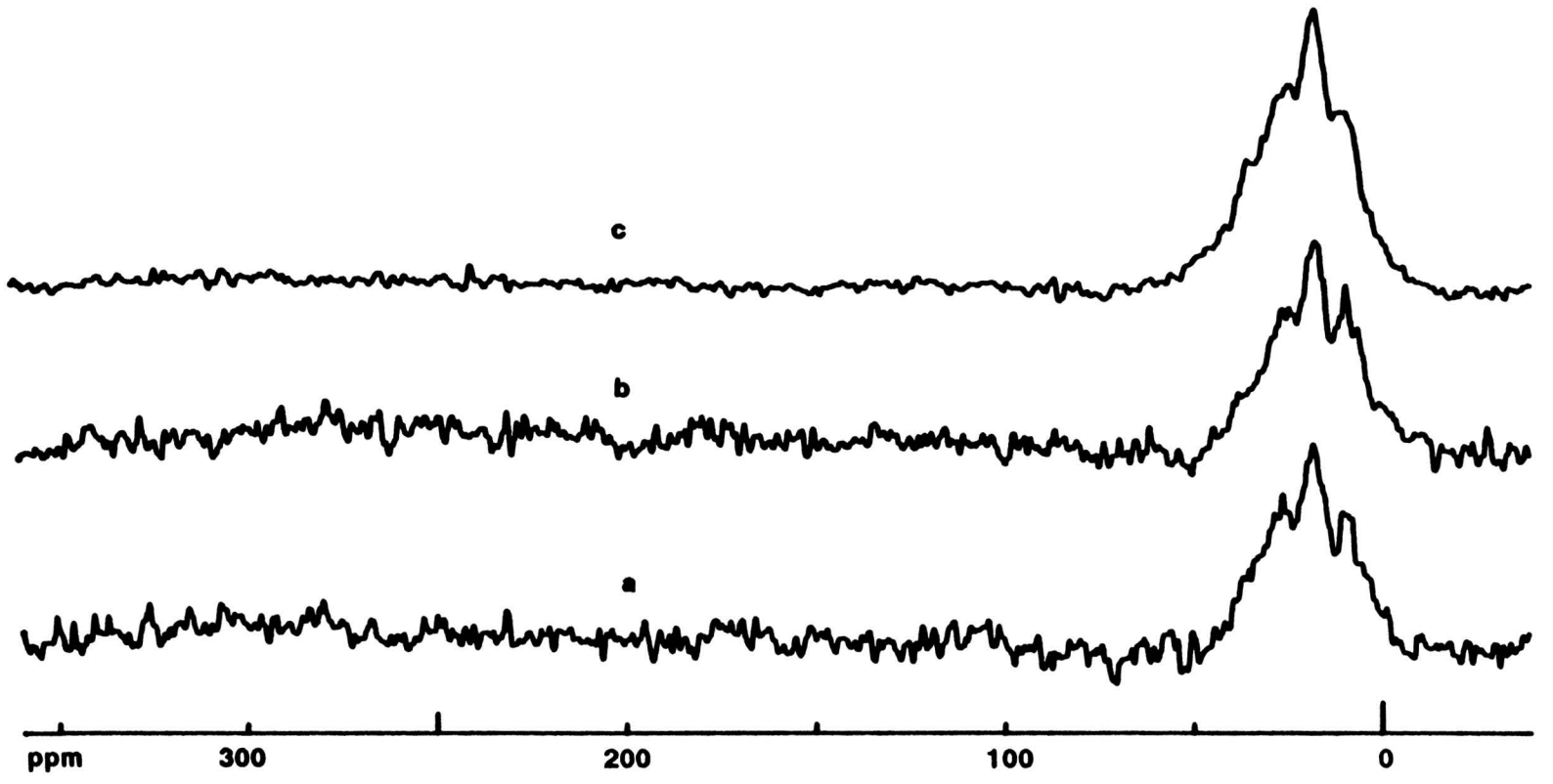

Figure 3.27 ^{13}C spectra of 2-propanol flowing over H-ZSM-5 at 180^{o} after the flow to 2-propanol has been bypassed. a) 2,000 scans; 118-120 min. b) 2,000 scans; 124-126 min. c) 145-155 min.

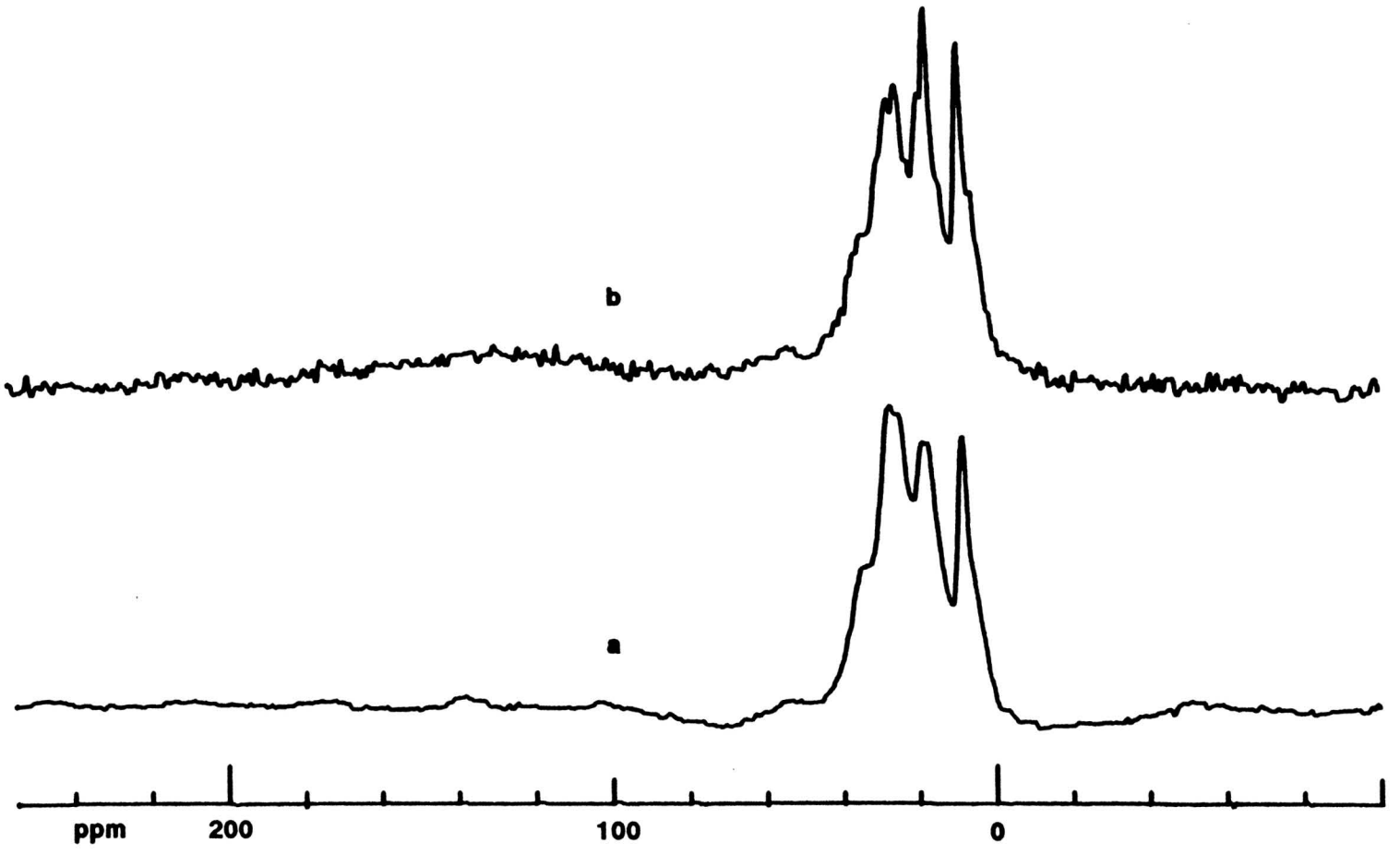

Figure 3.28 ^{13}C MAS solid state spectra of used catalyst from 180^{o} experiment. a) with cross polarization. b) no cross polarization.

restarted within the next hour. After restarting, the output of water and propene were significantly reduced and a greater amount of 2-propanol passed through the catalyst unreacted. Perhaps in the absence of the alcohol the oligomers reacted with each other thus blocking a greater number of acid sites.

The spectra of the non-labelled 2-propanol had very poor S/N even after many hours of flowing the alcohol and scanning up to 50,000 times per spectrum. Since the non-labelled alcohol was almost invisible to the NMR in our time frame, it made it convenient to use labelled then non-labelled 2-propanol to study the effect of the oligomerized material on the reaction. The apparatus was set up so that the labelled 2-propanol could be flowed until a steady-state built up and then the flow could be switched to non-labelled 2-propanol.

The experiment began when the stream of 2-propanol in nitrogen was introduced to the catalyst at 130°. Water immediately started coming off the catalyst but no signal was observed on the flowing NMR until a broad peak in the aliphatic region appeared after 50 minutes (Figure 3.29). The aliphatic region grew quickly during the next half hour but an alcohol peak was never seen (Figure 3.30). The alcohol was probably never seen because the alcohol bubbler used in this trial produced a smaller flow of 2-propanol and the alcohol reacted almost immediately after contacting the catalyst. The aliphatic region continued to visibly increase until about 220 minutes at which time it stayed constant or increased very slowly (Figure 3.31). Up to this time water was the only collected product. At about 240 minutes propene showed up in the gas chromatogram and in the ^{1}H NMR of the collected product stream (Figure 3.32). The isotopic ratio at the second carbon could be ascertained by comparing the area of the multiplets split by the ^{13}C versus the multiplet that was not split by the ^{12}C. The initial ^{13}C isotope concentration was about 90%. After about 290 minutes, the flow NMR, the gas chromatograms and the collected products appeared to be at a steady-state so the flow was switched to non-labelled alcohol (Figure 3.33). There were no apparent changes in the flow NMR during the next hour of the experiment (Figure 3.34). In an effort to see any small changes in the spectrum, a final spectrum of 100,000 scans was taken (Figure 3.35). No changes were apparent. The only change in the chromatograms was a tiny amount

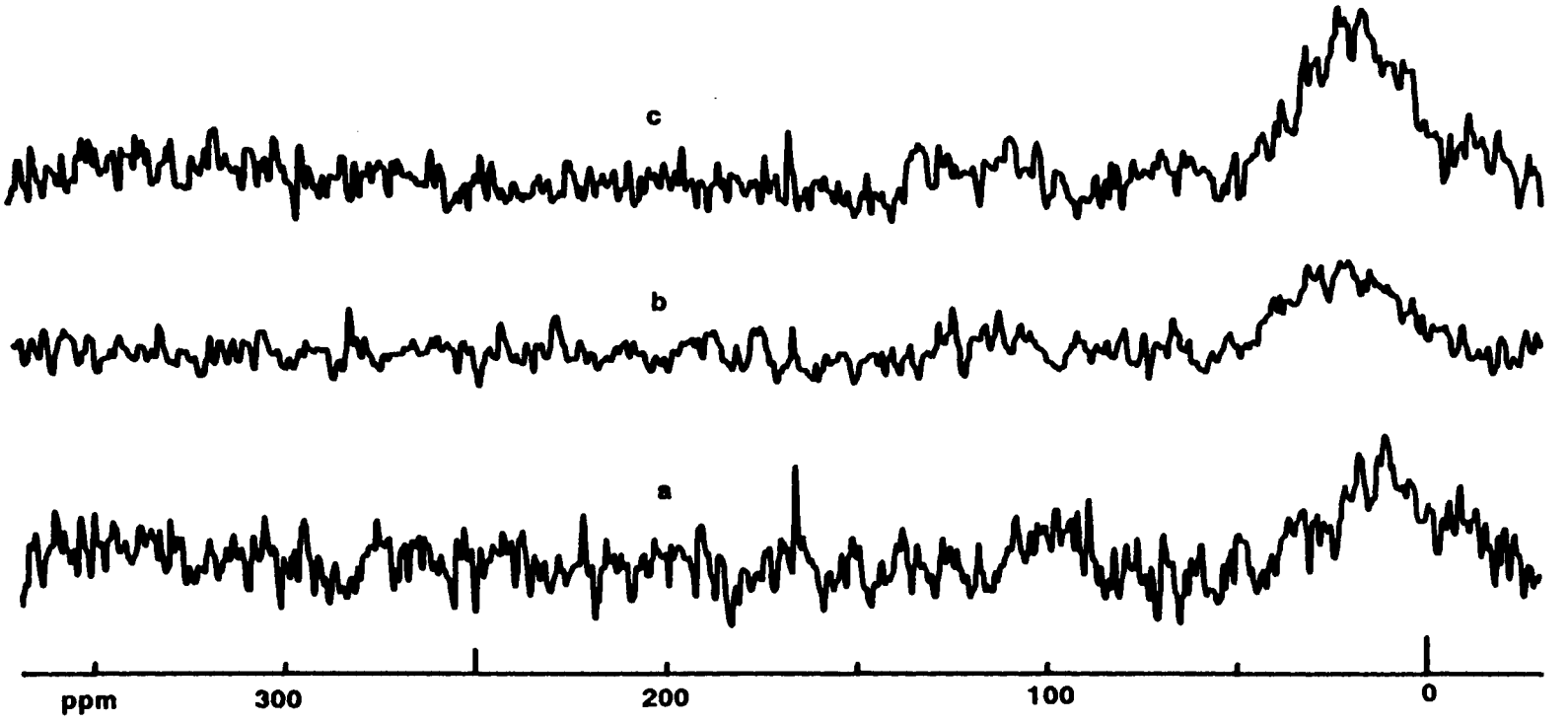

Figure 3.29 ^{13}C spectra of labelled/non-labelled 2-propanol flowing over H-ZSM-5 at 130^{o}. a) 43-53 min. b) 53-63 min. c) 64-74 min.

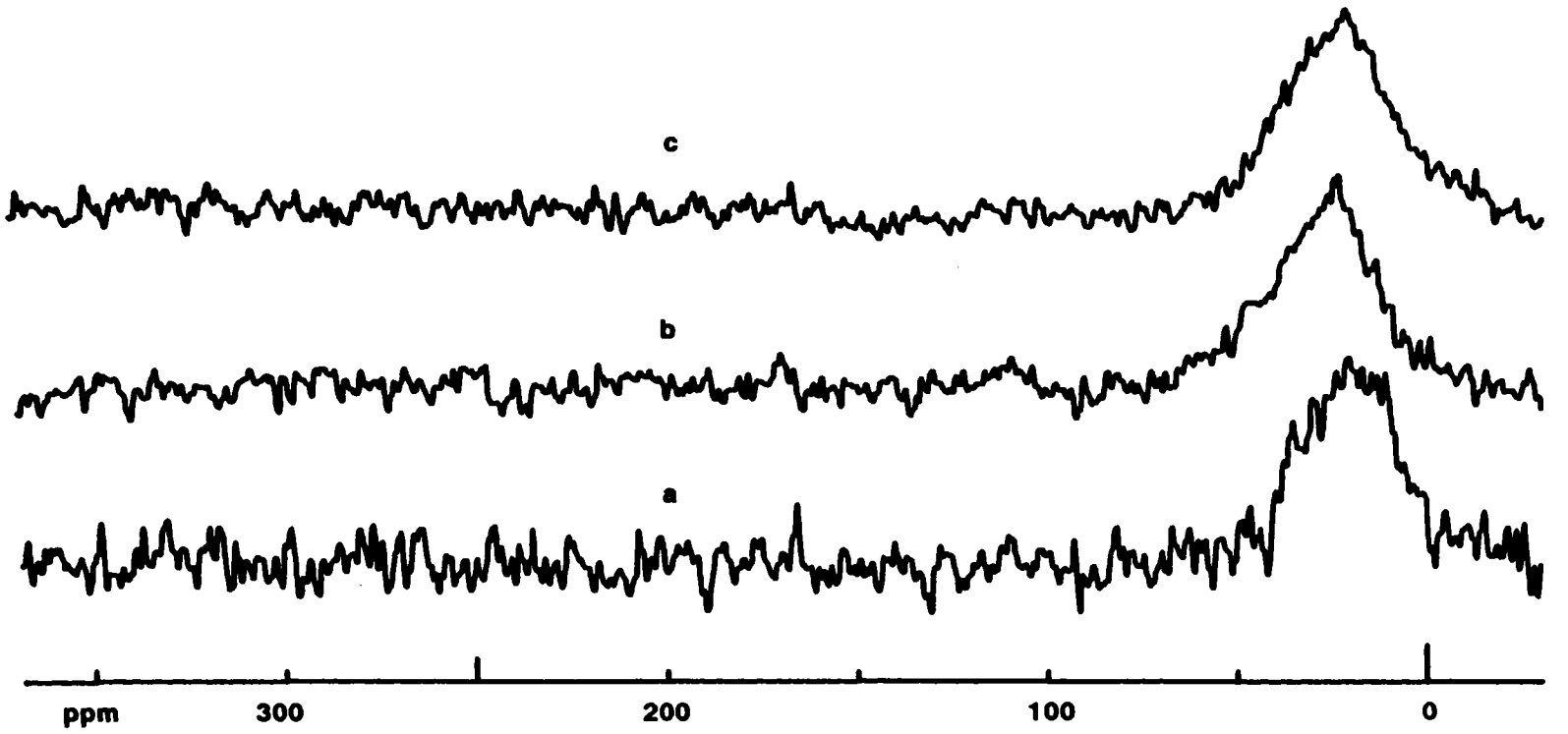

Figure 3.30 ^{13}C spectra of labelled/non-labelled 2-propanol flowing over H-ZSM-5 at 130^{o}. a) 74-84 min. b) 85-95 min. c) 95-105 min.

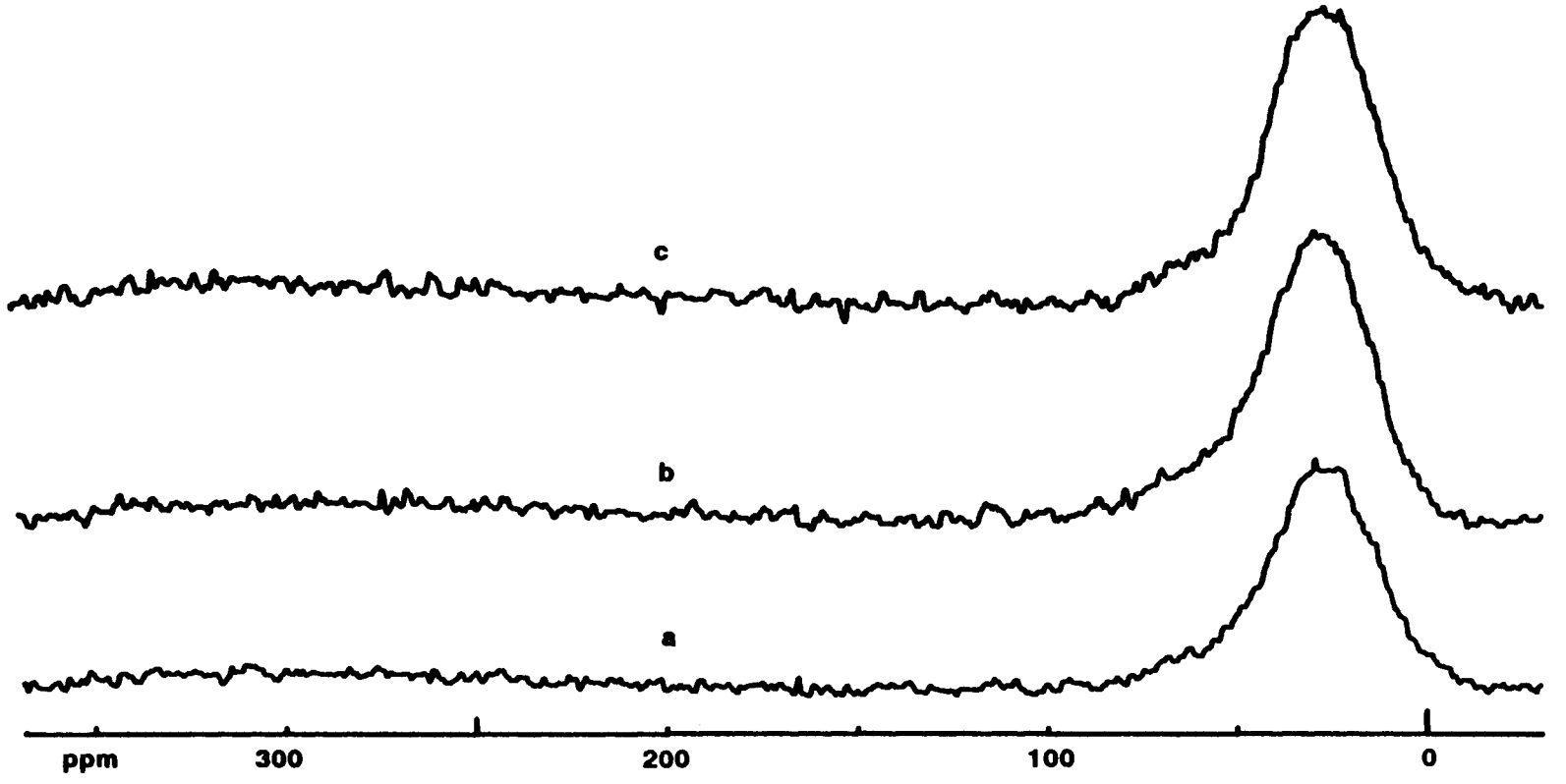

Figure 3.31 ^{13}C spectra of labelled/non-labelled 2-propanol flowing over H-ZSM-5 at 130^{o}. a) 211-221 min. b) 222-232 min. c) 232 -242 min.

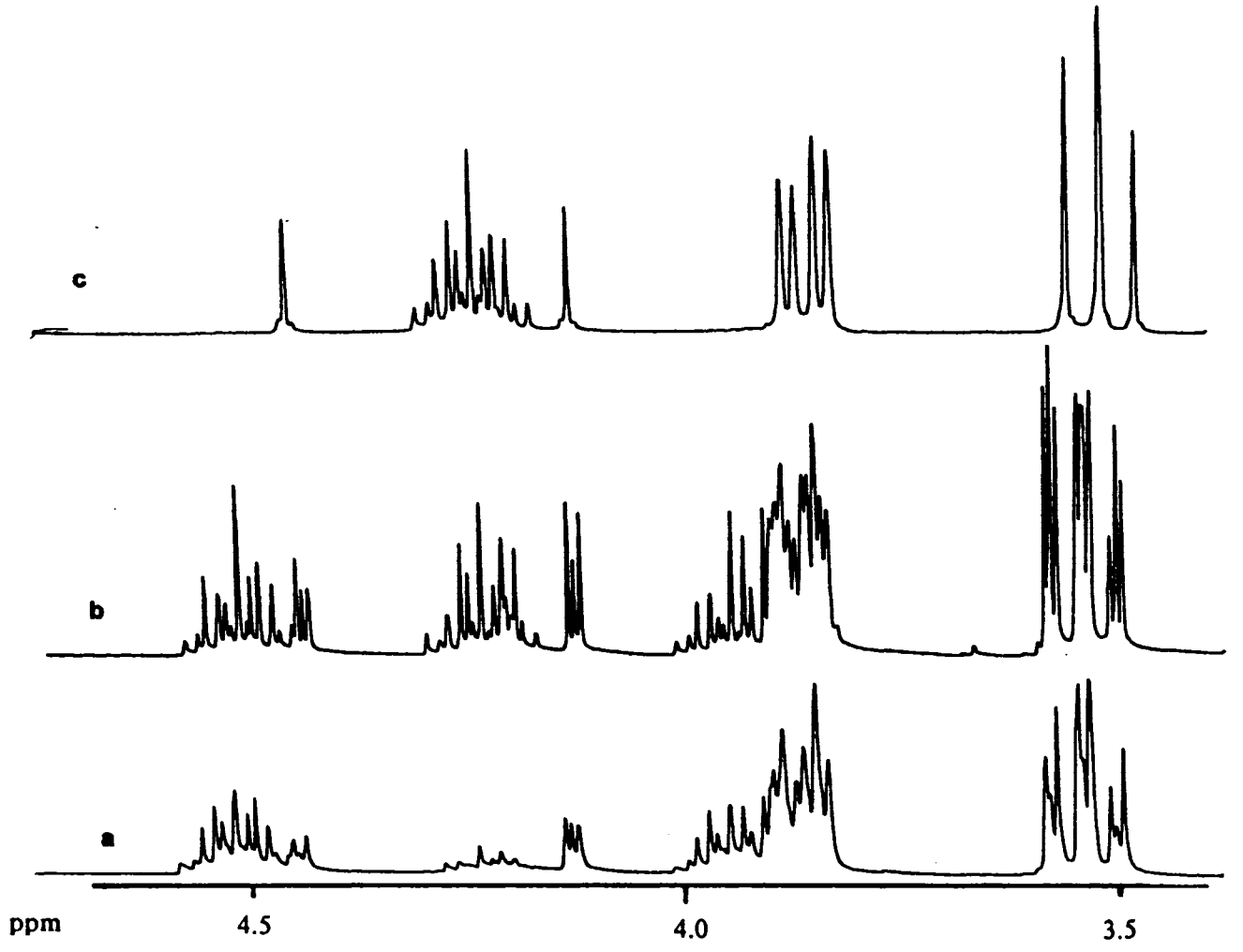

Figure 3.32 Expanded ^{1}H spectra of the collected products from labelled/non-labelled 2-propanol flowing over H-ZSM-5 at 130°. a) 261-271 min. b) 291-301 min. At 292 minutes 2-propanol was switched from labelled to non-labelled. c) 311-321 min.

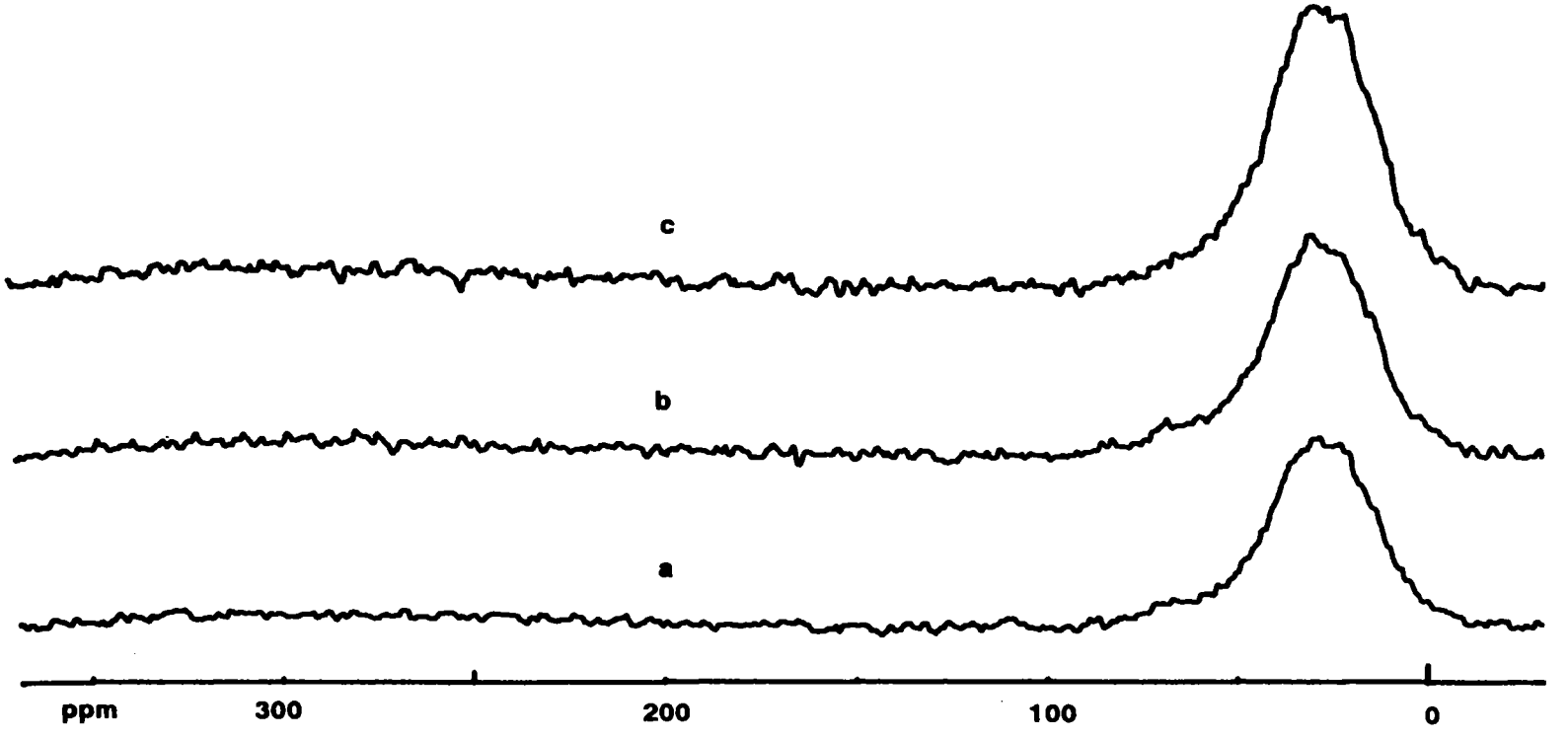

Figure 3.33 ^{13}C spectra of labelled/non-labelled 2-propanol flowing over H-ZSM-5 at 130^{o}. a) 276-286 min. b) 287-297 min. At 292 minutes 2-propanol was switched from labelled to non-labelled. c) 297-307 min.

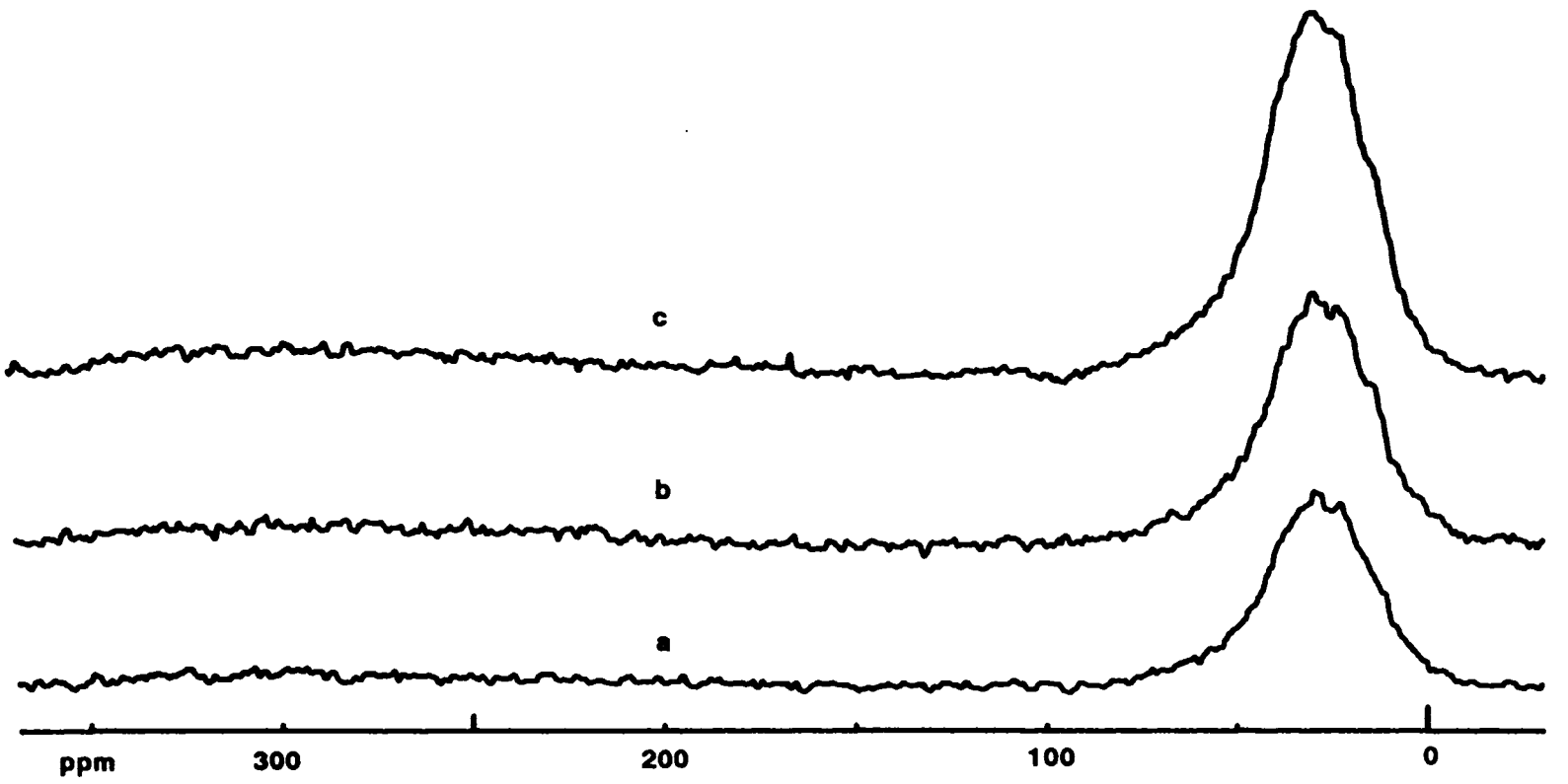

Figure 3.34 ^{13}C spectra of labelled/non-labelled 2-propanol flowing over H-ZSM-5 at 130^{o}. a) 308-318 min. b) 328-338 min. c) 348-358 min.

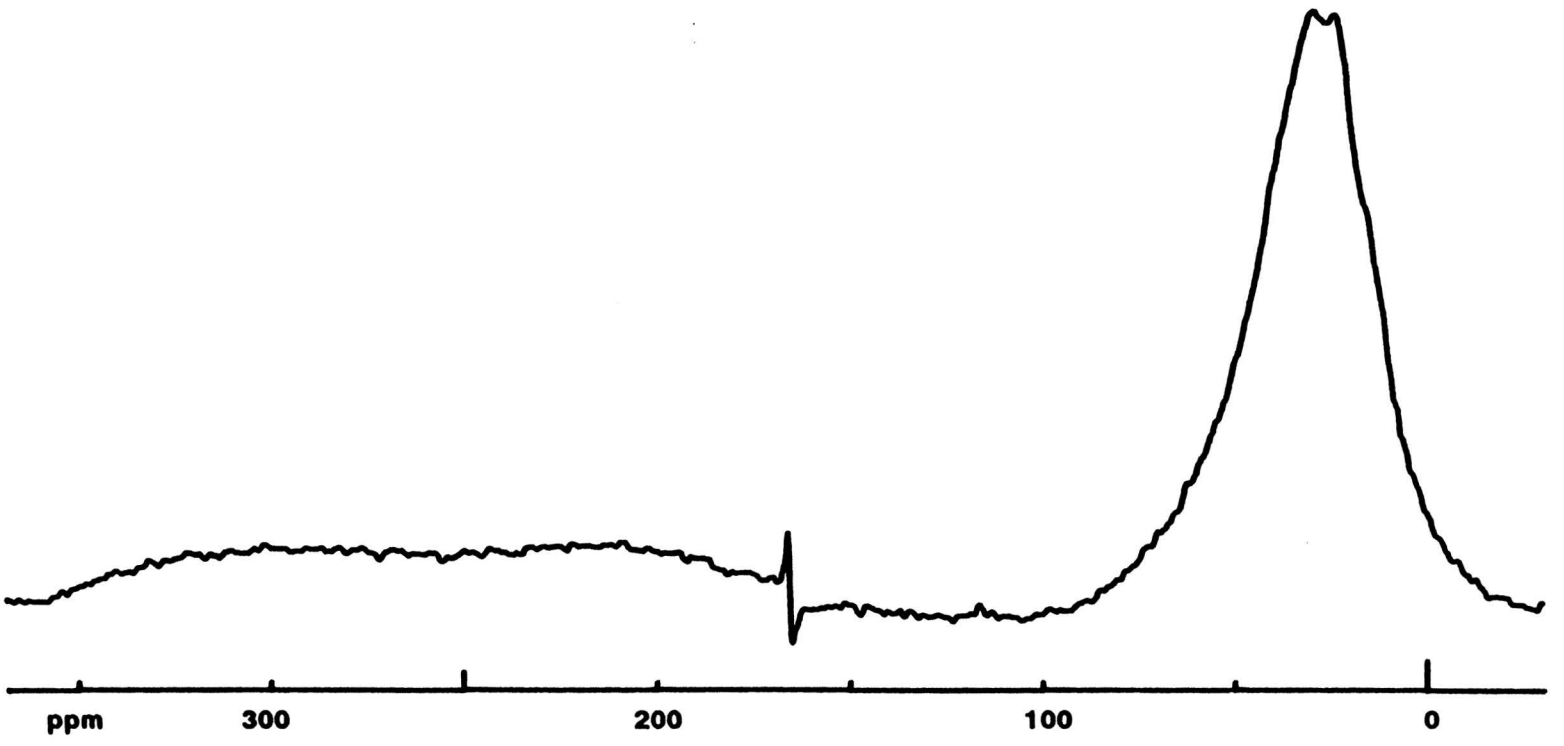

Figure 3.35 ^{13}C spectrum of labelled/non-labelled 2-propanol flowing over H-ZSM-5 at 130^{o}. 100,000 scans. 425-525 min.

of 2-propanol coming off the catalyst. The ^{1}H NMR of the products confirmed that virtually no interaction with the labelled oligomer took place because there was no labelled 1,2-dibromopropane in the product stream within 20 minutes after switching the label (Figure 3.32). Although there was no interaction at this temperature it is likely that at higher temperatures there would be some interaction. It is not known why the peak in the aliphatic region did not display the fine structure displayed in the other experiments. One contributing factor to the decrease in resolution was the reshaping of the rf coils after they had been damaged previous to this experiment.

Summary of reactions of 2-propanol on H-ZSM-5

By combining the results of the various trials, a possible picture of the dehydration of 2-propanol emerges. All aspects of this summary have not been proven, but the hypotheses are consistent with our results. At temperatures around 100°, the alcohol adsorbs on the Bronsted acid sites and ejects a water molecule. This may form an intermediate that is exchanging between a carbenium ion and an alkoxide with the lattice. The carbenium has not been observed but all of the chemistry is consistent with a carbenium ion. This intermediate may then either deprotonate and liberate propene or collide with another 2-propanol molecule and form diisopropyl ether. We only see diisopropyl ether below 130° because at higher temperatures the intermediate lifetime would be shorter which would decrease the chance of collision. As the temperature increases the intermediate is more likely to deprotonate and form propene. The intermediates are very reactive at this temperature and will readily react with propene to form oligomers. Once the oligomerization reaches a certain level then propene will exit the catalyst either due to blocking of the acid sites or by changing the nature of the acid site. At 130° the oligomer undergoes some branching and methyl shifts which scramble the label of the oligomer. As the temperature approaches 180° processes which require a higher activation energy such as linearization and cracking of the oligomer begin to occur.

CONCLUSION

The results from the flow NMR of H-ZSM-5 are valuable in two respects. Primarily, since this was the first reported in situ monitoring of a catalyst by flow NMR, we have demonstrated the efficacy and simplicity of the technique. Our results should encourage the application of this type of experiment to other catalytic systems, or to the study of other nuclei such as ^{19}F, ^{31}P. Secondly, we have shed light on the mechanism of dehydration of 2-propanol on H-ZSM-5. We have shown that at 130° C the dehydration does not go through a cyclopropyl carbenium ion transition state, propene oligomerizes on the catalyst and deactivates the catalyst before propene exits the catalyst, and the built up oligomer does not interact with newly introduced alcohol.

While the dehydration mechanism is better understood, we have still not spectroscopically observed a carbenium ion or alkoxy intermediate. If these two species are exchanging or reacting rapidly at over 100° C, then we will probably never see them unless we can monitor the reaction at a steady-state condition for many hours. It may be possible to observe these type of intermediates if we use lower temperatures and/or other reactant molecules that would produce a more stable carbenium ion. An alternative to monitoring ^{13}C would be to use an ^{17}O labelled alcohol. The number of ^{17}O resonances would provide valuable information even if the peaks could not be unambiguously assigned.

During the course of this project, several improvements in the experimental design were: addition of an internal standard, monitoring of the products with gas chromatography, and the addition of a bubbler that could sequentially introduce two different species into the system. While the flow NMR method we demonstrated was effective, there are other related systems that might improve upon our results: 1) Using a wide bore magnet so the amount of sample could be increased. 2) NMR spatial imaging of the catalyst bed by either moving the bed or by using field gradients. 3) Dynamic nuclear polarization (DNP) of the flowing reactants. 4) Dual mapping of reactant molecule and non-reactant molecule (N_2 or Xe). This technique would be particularly effective for ^{129}Xe if combined with DNP because of the high theoretical enhancements with xenon.

Literature Cited

(1) Davis, M. E.; Hathaway, P.; Morgan, D.; Glass, T.; Dorn, H. *Catalysis 1987* **1988**, 263.

(2) *Encyclopedia Britannica* 15th edition, Encyclopedia Britannica. 1139.

(3) Breck, D. *Zeolite Molecular Sieves*; John Wiley and Sons: New York, 1974; pp 1-28.

(4) *Encyclopedia of Materials Science and Engineering;* Pergamon: Elmsford, N. Y., 1986; vol 7, p 5511.

(5) Argauer, R. J.; Landolt, G. R. U. S. Patent 3,702,886, 1972.

(6) Jacobs, P. A. *Synthesis of High-Silica Alumino-silicate Zeolites*; Elsevier: Amsterdam, 1987.

(7) Michiels, P.; DeHerdt, O. C. E. *Molecular Sieve Catalysts*; Pergamon: Elmsford, N.Y., 1987; p 101-106.

(8) Van der Gaag, F. J.; Jansen, J. C.; Van Bekkum, H. *Appl. Catal.* **1985**, 17, 261.

(9) Kokotailo, G. T.; Fyfe, C. A.; Kennedy, G. J.; Gobbi, G. C.; Strobl, H.; Pasztor, C. T.; Barlow, G. E.; Bradley, S. In *New Developments in Zeolite Science and Technology*; Murakami, Y.; Iijima, A.; Ward, J. W., Eds.; Elsevier: Amsterdam, 1986; pp 361-368.

(10) Bolis, V.; Vedrine, J. C.; Van den Berg, J. P.; Wolthuizen, J. P.; Deroune, E. G. *J. Chem. Soc. Fara. Trans. I* **1980**, 76, 1606.

(11) Grady, M. C.; Gorte, R. J. *J. Phys. Chem.* **1985**, 89, 1305.

(12) Ghosh, A. K.; Kydd, R. A. *J. Catal.* **1986**, 100, 185.

(13) Anderson, J. R.; Mole, T.; Christov, V. *J. Catal.* **1980**, 61, 477.

(14) Zardkoohi, M.; Haw, J. F.; Lunsford, J. H. *J. Am. Chem. Soc.* **1987**, 109, 5278.

(15) Aronson, M. T. PhD Dissertation, University of Pennsylvania, 1987.

(16) Haw, J. F.; Richardson, B. R.; Oshiro, I. S.; Lazo, N. D.; Speed, J. A. submitted for publication in *J. Am. Chem. Soc.*

(17) Fraissard, J. *J. Chem. Phys.* **1982**, 76, 5225.

(18) Springuel-Huet, M. A.; Ito, T.; Fraissard, J. In *Structure and Reactivity of Modified Zeolites*; Jacobs, P. A.; Jaeger, N. I.; Jiru, P.; Kazansky, V. B.; Schulz-Ekloff, G., Eds.; Elsevier: Amsterdam, 1984; pp 13-21.

(19) Fraissard, J.; Ito, T.; Springuel-Huet, M.; DeMarquay, J. In *New Developements in Zeolite Science and Technology*; Murakami, Y.; Iijima, A.; Ward, J. W., Eds. Elsevier: Amsterdam, 1986; pp 393-400.

(20) Fyfe, C. A. *Solid State NMR For Chemists* C. F. C.: Ontario, Canada, 1983; Chapter 1.

Literature Cited (cont.)

(21) Suryan, G. *Proc. Indian Acad. Sci.* **1951**, A33, 107.

(22) Singer, J. R. *Science* **1959**, 130, 1652.

(23) Morse, O. C.; Singer, J. R.; *Science* **1970**, 170, 440.

(24) Grover, T.; Singer, J. R. *J. Appl. Physics* **1971**, 42(3), 928.

(25) Hahn, E. L. *Phys. Rev.* **1950**, 80, 580.

(26) Carr, H. Y.; Purcell, E. M. *Phys. Rev.* **1954**, 94, 630.

(27) Fyfe, C. A.; Cocivera, M.; Damji, S. W. H.; Hostetter, T. A.; Sproat, D.; O'Brien, J. *J. Mag. Reson.* **1976**, 23, 377.

(28) Fyfe, C. A.; Damji, S. W. H.; Koll, A. *J. Am. Chem. Soc.* **1979**, 101, 951.

(29) Fyfe, C. A.; Damji, S. W. H.; Koll, A. *J. Am. Chem. Soc.* **1979**, 101, 956.

(30) Buddrus, J.; Herzog, H.; Cooper, J. W. *J. Mag. Reson.* **1981**, 42, 453.

(31) Haw, J. F.; Glass, T. E.; Dorn, H. C. *Anal. Chem.* **1981**, 53, 2332.

(32) Bayer, E.; Albert, K.; Nieder, M.; Grom, E.; Wolff, G.; Rindlisbacher, M. *Anal. Chem.* **1982**, 54, 1747.

(33) Buddrus, J.; Herzog, H. *Org. Mag. Reson.* **1981**, 15(2), 211.

(34) Glass, T. E.; Dorn, H. C. *J. Mag. Reson.* **1983**, 51, 527.

(35) Glass, T. E.; Dorn, H. C. *J. Mag. Reson.* **1983**, 52, 518.

(36) Haw, J. F.; Glass, T. E.; Dorn, H. C. *J. Mag. Reson.* **1982**, 49, 22.

(37) Zhernovoi, A.; Latyshev, G. *Nuclear Magnetic Resonance in Flowing Liquids* Consultants Bureau, New York, **1965**.

(38) Silverstein, R. M.; Bassler, G. C.; Morrill, T. C. *Spectrometric Identification of Organic Compounds*; John Wiley and Sons: N.Y., **1981**; p 271.

(39) Gentry, J. J.; Rudham, R. *J. Chem. Soc. Fara. Trans. I* **1974**, 70, 1685.

(40) Nagy, J. B.; Lange, J. P.; Gourgue, P.; Bodart, P.; Gabelica, Z. In *Catalysis by Acids and Bases*; Imelik, B.; Naccache, C.; Coudurier, G.; Ben Taarit, Y.; Vedrine, J. C., Eds.; Elsevier: Amsterdam, **1985**; p 127.

(41) Winton, J.; Hunter, D.; Savage, P.; Ushio, S.; Schwartz, J.; Graff, G.; Cannon, D. *Chemical Week*, **1986**, 138(26), 20-71.

The vita has been removed from the scanned document